A novel glia-immune humanized mouse model for investigating neuroimmune mechanisms in CNS HIV infection and diverse neurological disorders

Shallu Tomer*[1], Lin Pan*[2], Jeffrey Harding[1], Valerie Rezek[1], Mitchell Krawczyk[2], Ethan Cook[1], Nandita Kedia[1], Li Wang[1], Jonathan Le[1], Christopher Platt[1], Heather Martin[1], Erik Gramajo[1], Xiang Li[2], Yewen Zhang[2], Ariel S. Peng[2], Yi Lu[2], Wenli Mu[1], Jing Wen[3], Scott Kitchen[1], Ye Zhang[§2] & Anjie Zhen[§1]

[1] Division of Hematology and Oncology, David Geffen School of Medicine, University of California, Los Angeles

[2] Department of Psychiatry and Biobehavioral Sciences, David Geffen School of Medicine, University of California, Los Angeles

[3] Depart of Department of Microbiology, Immunology, & Molecular Genetics, University of California, Los Angeles

*Co-first authors

[§]Corresponding Authors: Anjie Zhen, azhen@mednet.ucla.edu, Ye Zhang, yezhang@ucla.edu

Abstract

Dysregulation in neuroimmune interactions drives pathology in diverse neurological disorders. However, human cell-based in vivo models are limited for clinically relevant mechanistic studies and drug testing. To address this, we developed a novel humanized mouse model integrating all four major types of human glia - astrocytes, oligodendrocyte precursor cells (OPCs), oligodendrocytes, and microglia - in the brain, alongside donor-matched human immune system in peripheral blood and lymphoid tissues. We applied this model to study HIV-associated neurocognitive disorders, which can persist in tissue reservoirs including in the brain despite viral suppression by antiretroviral therapy. These glia-immune humanized

mice supported robust HIV-1 replication in the peripheral blood, lymphoid tissues, and the brain, and recapitulated the synapse loss observed in patients. Furthermore, HIV-infected mice exhibited heightened inflammation in both peripheral and brain tissues. Notably, OPCs and oligodendrocytes in HIV-infected brains adopted an immune activated phenotype, upregulating interferon-stimulated genes, highlighting understudied roles of oligodendroglia in HIV infection. RNA-sequencing of human glia identified the upregulation of inflammasome-associated genes and the downregulation of genes involved in transcriptional, epigenetic, and metabolic regulation. Overall, this model provides a powerful in vivo platform to investigate human neuroimmune interactions relevant to diverse neurological disorders, offering critical insights into HIV CNS infection, pathology, and potential therapeutic strategies targeting CNS reservoirs and neuroinflammatory pathways.

33 **Introduction**

34 Neuroinflammation, glial dysfunction, and immune dysregulation are key drivers of disease progression
35 in a variety of neurological disorders, including Alzheimer's disease (AD), Parkinson's disease (PD),
36 Huntington's disease (HD), stroke, and HIV-associated neurocognitive disorder (HAND)[1,2]. Despite their
37 critical roles and potential as therapeutic targets, investigation of neuroimmune dysfunction is among the
38 most challenging research areas, largely due to the lack of clinically relevant *in vivo* models. Human and
39 mouse glia are more distinct in transcriptome than their neuronal counterparts [3,4]. They react differently
40 to key pathological features of neurological diseases, such as exacerbated neuroinflammation and
41 oxidative stress[3]. Similarly, human and mouse immune cells diverge in significant ways. Consequently,
42 conventional mouse models do not capture human-specific features of the neuro-immune systems. The
43 vast majority of drugs identified in mouse models fail in clinical trials, severely delaying progress. While
44 human iPSC-derived in vitro cultures are useful for investigating one or several types of human cells,
45 they lack the full collection of glia and immune cell types and do not reproduce key anatomical structures
46 such as the blood-brain barrier. Humanized mouse models incorporating specific human immune and
47 glial cells have shown promise for investigating the functions and dysfunctions of these human cell types
48 *in vivo* [5-9]. However, none of the current humanized mouse models integrate all major human immune
49 and glial cell types. This represents a critical limitation, as resident glial cells and infiltrating immune cells
50 continuously interact and mutually influence each other's behavior, with these interactions being essential
51 determinants of neuroinflammation outcomes, disease progression, and brain repair. Thus, the
52 development of a humanized mouse model encompassing HLA-matched full complement of human glial
53 and immune cell types would provide an indispensable platform for mechanistic studies of human
54 neuroimmune interactions in vivo and for preclinical testing of therapeutics across a range of neurological
55 disorders.
56

57 Despite development of effective combined anti-retroviral therapy (ART), HIV remains largely incurable
58 due to persistent viral reservoirs, including in the central nervous system (CNS). As many as 50% of
59 people living with HIV (PLWH) experience CNS comorbidities [10]. Compared to peripheral reservoirs, our
60 understandings of the infection and reservoirs in the CNS are limited. Pathogenesis of HIV infection in
61 the CNS is multifactorial: HIV replicates and persists in the CNS resident cells, viral proteins are
62 neurotoxic, CNS inflammation occurs and many other pathogenic effects are observed. While microglia
63 appear to be the main HIV-1 reservoir in the brain[11], astrocytes and oligodendroglia - including
64 oligodendrocytes and oligodendrocyte precursor cells (OPCs) - may also be affected[12-14]. Astrocytes are
65 essential for brain homeostasis and can drive the induction and progression of a pro-inflammatory
66 environment. Damage to oligodendroglia and myelin has been detected in patients with HIV, correlating
67 with neurocognitive deficits [14,15]. Therefore, understanding how infiltrating immune cells and resident CNS
68 glia - microglia, astrocytes, and oligodendroglia - support and respond to HIV infection is critical for
69 elucidating the pathogenesis of CNS comorbidity.
70
71 Commonly used platforms for studying HIV CNS infection and pathogenesis have limitations. HIV does
72 not productively infect mice or non-human primates (NHPs)[16], and obtaining HIV-infected human brain
73 tissues from people living with HIV (PLWH) is challenging. As a result, the molecular mechanisms of HIV
74 CNS infection and CNS pathogenesis remain largely elusive. Humanized mice transplanted with human
75 hematopoietic stem cells (HSCs) allow the development of a functional human immune system, support
76 robust HIV replication, and enable HIV latency establishment[17-22]. These models have proven valuable
77 for investigating HIV immunopathogenesis, latency reactivation and testing gene and cell therapies as
78 described in ours[17-19,23-28] and others' studies[17,19,20,27-33]. However, available models, including new
79 humanized mouse models that contain injected astrocyte[34], or express human IL-34 to support better
80 development of microglia-like cells[34-37], do not include all four types of human CNS glia (microglia,
81 astrocytes, OPCs, and oligodendrocytes) and donor-matched human immune cells.
82

83 While much of HAND research has traditionally focused on neurons, and more recently on microglia and
84 astrocytes, oligodendroglia have been largely overlooked. In PLWH, abnormalities in white matter, where
85 oligodendrocytes and myelin are enriched, is a prominent neuropathological feature observed in both
86 pre- and post-ART eras and is associated with cognitive impairment[38]. Viral proteins such as Tat and
87 gp120 and neuroinflammation impair oligodendrocyte maturation and survival, while HIV-induced
88 neuroinflammation exacerbates demyelination and inhibits remyelination[13,14]. Recent scRNAseq studies
89 of postmortem human brain tissues from ART-treated PLWH also revealed significant transcriptomic
90 changes in OPCs [39]. However, previous mechanistic studies of CNS HIV infection have primarily relied
91 on in vitro cell cultures and transgenic mouse models that overexpress individual HIV proteins, such as
92 Tat or gp120 [40,41]. It is challenging to capture the full dynamics of viral replication, latency, and immune
93 interactions seen in human infection using these approaches, as they focus on isolated proteins at
94 artificially high levels - more akin to severe HIV encephalitis, which has become increasingly rare in the
95 ART era. Consequently, little is known about how HIV impacts OPC and oligodendrocyte function in vivo.
96
97 To address these critical knowledge gaps, we applied our novel glia-immune humanized mice to
98 investigate HIV CNS comorbidities. These glia-immune humanized mice support robust HIV infection in
99 both the periphery and the CNS. Chronic immune activation and neuroinflammation are strongly
100 associated with increased incidence of HAND[42]. Consistent with this, we observed elevated inflammation
101 and significant transcriptomic changes in human glia cells within the brains of infected mice, including
102 elevated type I interferon (IFN-I) responses, which mimic human conditions. Notably, OPCs and
103 oligodendrocytes in HIV-infected brains adopted an immune activated phenotype, upregulating
104 interferon-stimulated genes, highlighting understudied roles of oligodendroglia in HIV infection. Our
105 model provides a unique platform to investigate the interplay between HIV infection, chronic immune
106 activation, and neuroinflammation within a physiologically relevant humanized CNS environment. Beyond
107 HAND, this novel humanized mouse model will be an indispensable tool for mechanistic investigation of

108 neuroimmune interactions and preclinical therapeutic testing in a broad spectrum of neurological
109 disorders, including AD, PD, HD, stroke, and brain tumors.
110
111 **Results**
112 **The glia-immune humanized NSG mouse model supports the development of human multilineage**
113 **immune cells**
114 To study neuroimmune interactions in HIV CNS infection and other diseases and the role of human glia
115 in CNS inflammation, we developed a novel glia-immune humanized mouse model. In this model, mice
116 are reconstituted with donor-matched human glial cells in the brain and a human immune system in
117 periphery and lymphoid tissues. As shown in **Fig. 1A**, neonatal immunodeficient NSG mice (NOD.Cg-
118 *Prkdc*^{scid}*Il2rg*^{tm1Wjl}/SzJ) were injected with donor-matched gestation week <18 liver-derived CD34+ HSCs
119 (via intrahepatic injection) and brain-derived astrocytes and OPCs (via intracranial injection, as detailed
120 in[3]). For glial transplantation, astrocytes and OPCs were injected into the neonatal mouse brain at 4
121 injection sites, including the striatum and thalamus bilaterally. Mice were bled and the reconstitution level
122 was assessed 14-18 weeks after transplant.
123
124 We first determined whether glia-immune humanized mice exhibit similar levels of human immune
125 reconstitution when compared to primary human peripheral blood mononuclear cells (PBMCs) from
126 healthy donors and the Bone marrow- Liver-Thymus (BLT) humanized mouse, a well characterized
127 humanized mouse model that supports robust immune reconstitution and allows for comprehensive
128 studies in HIV immunity. The BLT humanized mouse model is key for seminal studies of cell and gene
129 therapy for HIV cure[8,18,20,43-54], studies in HIV latency[21,22,55,56] and mechanistic studies of HIV
130 immunopathogenesis [27,51,52,57-61]. We performed a comparative analysis among humanized glia-immune
131 mice, BLT mice, and fresh human PBMCs of the percentage of human leukocytes (CD45+ cells) in the
132 PBMCs and the distribution of human immune cell subsets, including T cells (CD3+), B cells (CD19+),
133 monocytes (CD14+) using flow cytometry.

134

135 In the glia-immune humanized mice, we observed similar level of CD45+% cells among the PBMCs as
136 compared to BLT mice **(Fig. 1B).** Within the human CD45+ leukocytes of the glia-immune mice, we
137 observed successful development of T cells (CD3+), B cells (CD19+) and monocytes (CD14+), at levels
138 similar to primary human PBMCs from healthy donors **(Fig 1C).** Glia-immune humanized mice showed
139 significantly better development of B cells and monocytes compared to BLT mice **(Fig 1C).** Among the T
140 cell subsets, 70.3% of T cells in the glia-immune humanized mice were CD4+ and 21.7% were CD8+,
141 similar to primary human PBMCs and to BLT mice **(Fig 1D).** These results suggest that glia-immune
142 humanized mice support robust development of multiple hematopoietic lineages, resembling human
143 PBMCs more closely than the humanized BLT mice.

144

145 **Reconstitution of human microglia-like cells, astrocytes, OPCs, and oligodendrocytes.**

146 To examine the reconstitution of human glia in host mouse brain, we performed IHC analyses of
147 xenografted mouse brains at 26 weeks post reconstitution. As shown in **Fig. 2A**, we observed widespread
148 engraftment of human glia in the brains, including astrocytes (hNuclei+Sox9+) (**Fig. 2D**), microglia-like
149 cells (huNuclei+Iba1+) (**Fig. 2E**), Oligodendroglia (huNuclei+Olig2+, **Fig 2F**), including OPCs (human
150 NG2+Olig2+, **Fig. 2G**), newly differentiated premyelinating oligodendrocytes (huNuclei+Bcas1+, **Fig. 2H)**,
151 and mature oligodendrocytes (huNuclei+ASPA+) (**Fig. 2I**) exhibiting a typical myelinating morphology
152 (**Fig 2J**). RNAscope confirmed the engraftment of human microglia-like cells (hCsf1r+) in the cerebral
153 cortex, hippocampus, and meninges (**Fig. 2C**), and human astrocytes (hSlc1a3+) in the cerebral cortex
154 (CTX), hippocampus (Hippo) and striatum (STR) (**Fig. 2B**). As shown in the quantification in **Fig. 2K-O**,
155 consistently high and widespread engraftment of human glial cells (astrocytes, microglia-like cells and
156 oligodendroglia) were observed in multiple brain regions, including the cortex, corpus callosum, and
157 striatum. Although we did not directly transplant human microglia, Iba1+Csf1r+ human microglia-like cells
158 were nonetheless detected in the xenografted mouse brains, likely originating from HSCs. The presence
159 of microglia-like cells, coupled with the widespread engraftment of human astrocytes and oligodendroglia,

160 establishes our model as a more comprehensive platform for neuroimmune research than traditional HSC
161 transplantation-based humanized mouse models, which do not contain the full complement of human
162 glia.
163
164 **Robust HIV replication and immune activation in glia-immune humanized mice.**
165 To examine if glia-immune humanized mice support robust HIV infection and induce peripheral activation,
166 mice were constructed and, following confirmation of successful immune reconstitution 14 weeks after
167 transplantation, were either left uninfected or infected with the R5 tropic HIV-1_{CH040} via intravenous
168 injection[17,18,25,26]. The levels of HIV replication over time were determined on plasma samples collected
169 at multiple time points post-infection (Weeks 2, 4, 6, 8, and 10). The viral load in the plasma showed a
170 progressive increase, with HIV RNA levels ranging from 1.2×10^6 copies/ml at Week 2 to 6×10^6
171 copies/ml at Week 10, demonstrating sustained viral replication over the 10-week observation period (**Fig.**
172 **3A**), similar to what was observed in the BLT humanized mouse model [62].
173
174 In addition to plasma, we assessed viral replication in lymphoid and CNS tissues. 10 weeks after HIV
175 infection, mice were euthanized and perfused with phosphate buffered saline (PBS), with the left
176 hemisphere of the brain fixed for IHC and RNAscope, while the right hemisphere was processed for flow
177 cytometry, real time PCR, and RNAseq analysis. HIV RNA was detected in the blood, spleen, and PBS-
178 perfused brain tissues using quantitative real-time PCR. The data revealed substantial HIV RNA
179 expression in all three tissues, with cycle threshold (Cq) values ranging from 26.34 to 42.20 in the blood,
180 20.18 to 30.12 in the spleen, and 26.46 to 33.37 in the brain. As shown in **Fig 3B**, the HIV-RNA analysis
181 was normalized to the expression level of housekeeping gene HPRT1. These findings confirm robust and
182 widespread HIV replication in both lymphoid tissues and the brain, indicating the model's suitability for
183 studying HIV dynamics in peripheral and CNS compartments.
184

185 HIV infection-mediated chronic inflammation is well documented in PLWH and in infected humanized
186 mice [24,27,63]. To assess whether glia-immune humanized mice exhibit HIV infection-induced chronic
187 inflammation, we used flow cytometry to analyze the expression of key activation marker CD38 and
188 exhaustion marker PD-1 on T cells from uninfected and infected glia-immune humanized mice. Activation
189 marker CD38 and exhaustion marker PD-1, were both markedly increased on CD4+ and CD8+ T cells in
190 the blood (**Fig 3C-F**) and the spleen (**Fig 3G-J**) of HIV infected mice as compared to uninfected mice.
191 These findings demonstrate that glia-immune humanized mice recapitulate key features of HIV
192 pathogenesis, including robust viral replication in peripheral and CNS compartments and chronic
193 peripheral immune activation, supporting the model's relevance for studying systemic and neuroimmune
194 consequences of HIV.
195
196 **HIV infection elevates type I IFN responses, and the "immune oligodendroglia" state in the CNS.**
197 HIV infection induces type I IFN responses in PLWH [64,65]. We and others have shown that chronic type I
198 IFN activation leads to chronic inflammation, T cell exhaustion, and maintenance of HIV reservoirs [9,25,48].
199 To examine whether glia-immune humanized mice exhibit type I INF response, a key mechanism for HIV
200 pathogenesis, we examined type I IFN response gene (ISG) MX1 expression by real-time PCR. We
201 observed that infected mice showed significantly elevated levels of MX1 in blood, spleen and brain
202 tissues compared to uninfected controls (**Fig. 4A**), mirroring observations in PLWH[66-68] and reflecting the
203 ongoing immune activation in response to persistent HIV replication. To identify molecular changes in
204 human glia in response to HIV infection, we performed bulk RNA-seq and analyzed transcripts mapped
205 to the *human* reference genomes using brain samples from HIV-infected versus uninfected mice. RNA-
206 seq revealed a striking induction of type I ISGs and associated antiviral pathways in human glial cells
207 from infected mice (**Fig. 4B-D**). Differential gene expression analysis (Volcano plot in **Fig. 4B**) identified
208 multiple significantly upregulated ISGs (e.g., OAS3, ISG15, IFI44, IFI44L, IFIT3) alongside classical
209 interferon-regulatory factors (IKZF2, IFNGR1), suggesting a heightened antiviral state in the HIV-infected
210 brain. Network analysis of differentially expressed genes (**Fig. 4C**) highlighted a large, interconnected

211 module of upregulated genes (red) enriched for interferon-associated factors, whereas a cluster of
212 downregulated genes (blue) encompassed components implicated in transcriptional regulation (ZNF652,
213 IKZF2), metabolism (ACSS2, DUT, STIM1) and epigenetic control (EP300). Consistent with these
214 observations, gene set enrichment analysis (**Fig. 4D**) demonstrated that upregulated genes were
215 significantly overrepresented in pathways related to “Interferon alpha/beta signaling”, “PKR-mediated
216 signaling”, and “ISG15 antiviral mechanisms”. Immunohistochemistry (IHC) further confirmed increased
217 IFN-I response gene human MX1 expression in the brains of infected mice (**Fig. 4E-I**). We observed
218 increased density of hMX1+ glial cells in corpus collosum, cortex, hippocampus and thalamus of the glia
219 immune humanized mice (**Fig.4G-I**). These results reveal molecular changes induced by HIV infection in
220 human glia in vivo, further demonstrating the value of the glia-immune humanized mouse model for
221 investigating the molecular mechanisms of HIV CNS infection and other neurological disorders.
222
223 To identify which CNS cell type(s) upregulate MX1 expression during HIV infection, we performed co-
224 immunostaining of MX1 with Iba1 (microglia-like cells), GFAP (astrocytes), Olig2 (OPCs and
225 oligodendrocytes), NG2 (OPCs), and CC1 (oligodendrocytes) (**Fig.4 J-M**). Surprisingly, we observed
226 more extensive colocalization of MX1 with Olig2, NG2, and CC1 (**Fig.4K-M**), whereas colocalization with
227 Iba1 or GFAP was minimal (**Fig 4J**). These findings suggest that oligodendroglia are the predominant
228 cell type upregulating MX1 expression in the HIV-infected brain. To assess potential regional
229 heterogeneity in MX1 expression among oligodendroglia, we quantified the percentage of MX1+ cells
230 among human oligodendroglia across different brain regions. We found a lower proportion of MX1+
231 oligodendroglia in the corpus callosum compared to the cortex and striatum (**Supplementary Fig. 1**),
232 suggesting that oligodendroglia from distinct brain regions differ in their susceptibility to adopting the
233 immune oligodendroglia state during HIV infection.
234
235 Interestingly, we observed a significant increase in ASPA+Olig2+ mature oligodendrocytes in the corpus
236 callosum (**Fig 5 A, C, D, F**) and striatum (**Fig 5G**). However, this increase was only evident when both

237 human and mouse cells were included in the quantification, whereas the densities of huNG2+ (human
238 OPCs), huNuclei+ASPA+ (human mature oligodendrocytes) or huNuclei+Olig2+ cells (all human
239 oligodendroglia) were unchanged (**Supplementary Fig. 2**). In contrast to the increase in mature
240 oligodendrocytes, densities of Bcas1+ immature oligodendrocytes remained unchanged (**Fig. 5B, E**).
241
242 Consistent with our observations, studies of postmortem patient tissue show elevated Interferon-
243 mediated signaling pathway in OPCs from HIV infected individuals[39,69]. Oligodendrocyte density was
244 shown to be elevated in patients with mild pathology while decreased in untreated patients who died of
245 AIDS[70,71]. Although oligodendroglia has traditionally been studied exclusively for their role in forming
246 myelin, emerging evidence indicates that OPCs and oligodendrocytes can acquire an immunomodulatory
247 phenotype. Here, our observation supports the presence of "immune OPCs" and "immune
248 oligodendrocytes" that have elevated IFN-I gene expression in HIV infected brains, highlighting
249 underappreciate roles of oligodendroglia in HIV CNS pathology.
250
251 **HIV infection leads to microglia and astrocyte reactivity and loss of synaptic proteins in glia-**
252 **immune humanized mouse.**
253 To determine if HIV infection disturbs brain homeostasis, we examined the status of microglia and
254 astrocytes in these mice. As key regulators of central nervous system homeostasis, microglia and
255 astrocytes function as the brain's primary immune responders. Increases in microglia marker Iba1 and
256 reactive astrocyte marker GFAP are often associated with neuroinflammation and neuropathology [72 73].
257 We quantified microglia density (Iba1+ cells) (**Fig. 6A**) and reactive astrocyte density (GFAP+ cells) (**Fig.**
258 **6B**) in four brain regions: the cortex, corpus callosum, hippocampus, and thalamus. Microglia density
259 significantly increased in the hippocampus and thalamus compared to control (**Fig. 6C-F**). Similarly, the
260 density of reactive astrocytes also increased in the corpus callosum and hippocampus compared to
261 control (**Fig. 6G-J**).
262

263 Synapse loss is a hallmark of HAND, and its extent correlates with cognitive impairment. To evaluate
264 synaptic changes, we conducted IHC for the presynaptic protein VGLUT2 and the postsynaptic protein
265 PSD-95. In the CA1 region of the hippocampus, HIV-infected mice exhibited a significant reduction in
266 VGLUT2 immunofluorescence compared to controls (**Fig. 6K&L**), whereas PSD-95 immunofluorescence
267 remained unchanged (**Fig. 6K&M**). These results suggest that our humanized mouse model recapitulates
268 HIV infection-associated synapse loss in patients, providing a valuable model for mechanistic study and
269 drug testing for HIV associated cognitive impairment.

270

271 **Discussion**

272 Previous humanized mouse models, which typically incorporate a single type or a limited subset of human
273 cells, have been instrumental for preclinical studies of disease mechanisms[7,48,74-87]. Building on these
274 foundations, the next-generation glia-immune humanized mouse model described here represents an
275 important advancement, enabling in vivo investigation of human neuroimmune interactions with greater
276 cellular complexity and physiological relevance. By integrating all four major types of human glial cells -
277 astrocytes, microglia-like cells, OPCs, and oligodendrocytes - alongside donor-matched peripheral
278 immune cells within the same mouse, this model recapitulates the complex cellular landscape and
279 intercellular interactions of the human CNS more faithfully than previous systems. For example, glial cells
280 present antigen but HLA-mismatched antigen presentation cells cannot properly engage with T cells and
281 may themselves be subject to immune rejection. Thus, establishing a humanized mouse model
282 incorporating HLA-matched, full complement of human glial and immune cell types would provide an
283 indispensable platform for human neuroimmune interaction studies.

284 Here, we demonstrated the value of this model for CNS HIV research. Current humanized mouse models,
285 while invaluable for studying peripheral HIV infection, have been limited in their utility to understand CNS

286 infection due to the lack of matched human glia in the brain. Glia, including microglia, astrocytes, OPCs,
287 and oligodendrocytes, are essential mediators of CNS homeostasis and immune responses, and their
288 dysfunction in the setting of HIV infection is implicated in neurological complications [13,88,89]. By
289 incorporating donor-matched glial cells, our model supports robust engraftment of astrocytes, OPCs,
290 oligodendrocytes, and microglia-like cells, and simultaneous robust peripheral immune reconstitution of
291 donor matched HSCs. Our model provides a unique platform to investigate HIV infection that spans
292 peripheral organs and the CNS.

293 Our data demonstrated that our model supports robust and persistent HIV replication in the peripheral
294 blood, lymphoid tissues and in the brain. The elevated proinflammatory gene expression in both the
295 periphery and brain underscores the potent immunopathological effects of HIV infection. Specifically,
296 RNA sequencing of brain tissues demonstrated upregulation of type I ISGs and inflammasome-
297 associated genes in human glial cells. Importantly, we observed glia reactivity in HIV infected animals,
298 including in oligodendroglia and astrocytes, which are not key reservoirs of HIV, suggesting that
299 bystander reactivity of glial cells may play key role in CNS inflammation and HAND[90]. Interestingly, in the
300 brains of infected glia-immune humanized mice, we also observed several down regulated genes that
301 are related to glia metabolism. For example, STIM1 is involved in calcium signaling, which is essential
302 for astrocyte and microglial responses to inflammatory stimuli[91,92]. Downregulation of STIM1 suggests an
303 impairment in calcium signaling pathways, potentially leading to glial dysfunction and contributing to
304 neuroinflammation[93]. Similarly, decreased ACSS2 levels could affect neuronal energy metabolism and
305 histone acetylation, impacting neuronal function and memory formation[94-96]. Therefore, our model offers
306 a powerful platform to investigate the molecular mechanisms of HIV-driven neuroinflammation and glial
307 dysfunction in the brain.

308 Our discovery that human OPCs and oligodendrocytes adopt an immune phenotype - marked by robust
309 upregulation of type I ISG MX1 expression in HIV-infected glia-immune humanized mouse brains
310 provides novel insights into the dynamic, immunomodulatory potential of human oligodendroglia in the

311 diseased CNS. These results complement reports of oligodendroglia damage in HIV infection[13,14,97-99].
312 Traditionally viewed primarily as myelinating cells and precursors, these findings position oligodendroglia
313 as active participants in neuroimmune responses, capable of sensing inflammatory cues and engaging
314 in immune signaling. Although immune oligodendroglia have been described in models of multiple
315 sclerosis and aging[100-102], their presence in the context of HIV infection has not, to our knowledge, been
316 previously reported. In HIV infection, this immune oligodendroglia state may contribute to
317 neuroinflammation and white matter damage in synergy with canonical immune cells such as microglia
318 and infiltrating macrophages and T cells. These observations raise the possibility that oligodendroglia
319 may serve as amplifiers or modulators of CNS inflammation in HAND and potentially in other
320 neuroinflammatory and/or demyelinating disorders. Future research should explore whether this immune
321 oligodendroglia phenotype is reversible, whether/how it contributes to impaired remyelination or neural
322 circuit dysfunction, and how it is regulated by specific inflammatory mediators or viral products. Our model
323 provides a novel platform for investigating the function of human immune oligodendroglia in vivo in a
324 range of neurological disorders and our findings point to human oligodendroglia as a previously untapped
325 therapeutic target in neuroimmune disorders.
326
327 The ability of this glia-immune humanized mouse model to recapitulate HIV infection and inflammation in
328 the CNS offers a valuable tool for testing curative and neuroprotective interventions. Our model supports
329 a full range of biochemical, imaging, and physiological techniques, creating a robust platform for
330 translational research on neuro-immune interactions in HIV CNS comorbidities and other CNS diseases.
331 In addition, throughout the seven-month study period, we did not observe graft-versus-host disease
332 (GVHD) in our glia-immune humanized mice, highlighting the stability and tolerability of the dual
333 transplant methods.
334
335 The survival of myeloid cells requires species-specific M-CSF[103]. Thus, previous methods for
336 reconstituting human myeloid cells in mice typically require transgenic expression of human M-CSF[75,80-

337 [82]. In our study, neonatal transplantation of human HSCs and glia is sufficient to maintain the survival of
338 some human myeloid cell in the blood and brain, suggesting that either the transplanted human cells and
339 their progeny produce M-CSF or the neonatal host mouse provides alternative growth factors that
340 compensate for the species-specific need for human M-CSF. In future studies, utilizing host mice that
341 express human M-CSF to construct glia-immune humanized models may further enhance the
342 engraftment and expansion of human myeloid cell populations.
343
344 In summary, our glia-immune humanized mouse model fills a critical gap in HIV research by integrating
345 donor-matched human glia and a functional human immune system. Our findings highlight the capacity
346 of these mice to support HIV replication within both peripheral and CNS tissues, mirroring key features
347 of human HIV neuropathogenesis. Beyond HIV research, such humanized mouse models hold
348 tremendous potential for advancing our understanding of other neurological diseases that involve
349 complex interactions between human glia and immune cells. There are many major differences between
350 human and mouse immunology in both innate and adaptive immune responses[104], and in glial cells[3,79].
351 Our model will enable the mechanistic dissection of neuroimmune signaling pathways, human glial-
352 immune crosstalk, and their roles in disease initiation and progression across a spectrum of neurological
353 disorders, including neuroinfectious diseases, demyelinating diseases, neurodegenerative disorders, and
354 neuroinflammatory conditions. Furthermore, this model provides a unique opportunity for the
355 development and pre-clinical testing of human immune therapies (such as antibody-based therapeutics
356 [105] or Chimeric Antigen Receptor therapy[106]) that modulate neuroimmune interactions in CNS disorders.
357 In future work, deeper single-cell analyses and spatial transcriptomic approaches can further delineate
358 the molecular interaction among astrocytes, OPCs, oligodendrocytes, microglia, neurons, and peripheral
359 immune cells during HIV infection.
360
361 **Materials and Methods**
362 **Isolation of human astrocytes and OPCs**

363 All mid-gestation tissue-related experiments were carried out in accordance with relevant federal, state,
364 and local laws, including adherence to required regulatory approvals and informed consent procedures.
365 Human glia were isolated from gw 18 brains using a protocol adapted from a rat glia enrichment
366 protocol[107]. Briefly, gw 18 brains were chopped into small pieces using a razor blade and enzymatically
367 dissociated with papain. Dissociated cells were plated in a T75 flask and maintained in a serum-
368 containing culture medium. Three days later, unwanted cells such as neurons were depleted by
369 mechanical shaking. Remaining attached cells, which contains both astrocytes and OPCs, were
370 maintained in culture until transplantation.
371
372 **Generation of glia-immune humanized mouse**
373 We developed a novel glia-immune humanized mouse model, where the mice were reconstituted with
374 donor-matched human glia in the brain and a human immune system in the peripheral and lymphoid
375 tissues. P2-6 immunodeficient NSG mice (NOD.Cg-Prkdc^scid Il2rg^tm1Wjl/SzJ) were injected with 0.5
376 million donor-matched, gestation <18 weeks liver-derived CD34+ HPSCs via intrahepatic injection and
377 400,000 brain-derived astrocytes and oligodendroglial cells via intracranial injection at four sites in the
378 subcortical regions of the brain, including the striatum and thalamus bilaterally[3]. Fourteen weeks post-
379 reconstitution, successful immune reconstitution was confirmed in the peripheral blood of the humanized
380 mice, with detectable levels of human T cells, B cells, and monocytes.
381
382 **Infection of mice and quantification of viral loads**
383 Glia-immune humanized mice were inoculated with HIV-1 CH040 [108] (500 ng of p24 per mouse) via retro-
384 orbital injection under general anesthesia. To assess HIV plasma viremia every two weeks, viral RNA
385 was extracted from plasma samples, and a one-step real-time PCR was conducted using the TaqMan
386 RNA-to-Ct 1-Step kit (Thermo Fisher Scientific, USA). PCR amplification was performed with the
387 following primers and probe:
388 CH040 forward primer: CAATGGCAGCAATTTTACCA

389 CH040 reverse primer: GAATGCCGAATTCCTGCTTGA

390 CH040 dye-labeled probe: 5' [FAM]- CCCACCAACAGGCGGCCTTCACTG-[NFQ]- 3'

391

392 **Nucleic acid isolation and real time PCR**

393 To assess the expression levels of the Type 1 interferon (IFN) response gene, MX1, and cell-associated
394 HIV RNA, RNA was extracted from harvested cells following the manufacturer's protocol (Qiagen). cDNA
395 was synthesized using the High-Capacity cDNA Reverse Transcription Kit (Thermo Fisher Scientific,
396 USA). For the quantification of MX1 and HPRT1, TaqMan Gene Expression Assays (Thermo Fisher
397 Scientific, USA) were used with the following probes: Human MX1 (Hs00895608_m1) and Human
398 HPRT1 (Hs01003267_m1). For HIV RNA quantification, the primers and probes specific to the CH040
399 strain, as described above, were utilized.

400

401 **Flow cytometry**

402 Single-cell suspensions prepared from the peripheral blood and spleen of glia-immune humanized mice
403 were stained with the following antibodies: CD45 (clone HI30), CD3 (clone OKT3), CD4 (RPA-T4), CD8
404 (RPA-T8), CD14 (clone 61D3), CD11c (clone 3.9), CD11b (clone ICRF44), CD19 (HIB19), PD-1 (clone
405 EH12.2H7), and CD38 (clone HIT2). To facilitate live cell gating, the LIVE/DEAD Fixable Yellow Dead
406 Cell Stain Kit (Invitrogen, USA) was used. Antibodies for cell surface markers were conjugated to a range
407 of fluorophores, including BV785, BV605, Pacific Blue, Alexa Fluor 700 (AF700), Phycoerythrin (PE),
408 ECD, PE-Cy7, Allophycocyanin (APC), PerCP-Cy5.5, and PE-Cy5 in appropriate combinations. Data
409 acquisition was performed using the LSR Fortessa flow cytometer and FACS Diva software (BD
410 Biosciences), while FlowJo software (version 10.7.2) was used for data analysis.

411

412 **IHC**

413 Glia-immune humanized mice were anesthetized with isoflurane and transcardially perfused with 1× PBS
414 (pH 7.4), followed by fixation with 4% paraformaldehyde (PFA). Brains were post-fixed in 4% PFA at 4 °C

415 overnight, then transferred to a 30% sucrose solution at 4 °C for two days or until they sank. Samples
416 were embedded in optimal cutting temperature (OCT) compound (Fisher, cat#23-730-571) and stored at
417 −80 °C until sectioning. Brain tissue was cut into 30 μm slices using a Leica cryostat and stored in
418 cryoprotectant solution (30% sucrose, 1% polyvinylpyrrolidone, and 30% ethylene glycol in 0.1 M
419 phosphate buffer) at −20 °C. For immunostaining, sections were blocked and permeabilized with 10%
420 donkey serum and 0.3% Triton X-100 in PBS, then incubated with primary antibody solutions overnight
421 at 4 °C. For human NG2 and Bcas1 staining, primary antibody incubation was extended to 2 days. Heat-
422 induced antigen retrieval was performed to reveal ASPA signals. Sections were first rinsed with antigen
423 retrieval buffer (10 mM sodium citrate, 0.05% Tween-20, pH 6.0) for 5 min at room temperature. They
424 were then transferred into pre-heated antigen retrieval buffer and subjected to heat-induced antigen
425 retrieval using a vegetable steamer for 10 min. After heating, sections were allowed to cool to room
426 temperature in the same buffer before proceeding to blocking and immunostaining. The following primary
427 antibodies were used: anti-human nucleus protein (Chemicon, cat#MAB1281, 1:500 dilution), anti-human
428 nuclei (Thermo Fisher, cat# PA5-18498, 1:500 dilution), anti-Iba1 (Wako, cat#019-19741, 1:500 dilution),
429 anti-Olig2 (Millipore, cat#211F1.1, 1:1000 dilution), anti-Sox9 (R&D, cat#AF3075, 1:1000 dilution), anti-
430 GFAP (Dako, cat# Z0334, 1:1000 dilution), anti-human MX1 (Abcam, cat#ab284603, 1:500 dilution), anti-
431 Bcas1 (Synaptic system, cat# 445 003, 1:250 dilution), anti-ASPA (Genetex, cat# GTX113389, 1:500
432 dilution), Anti-GST-π (MBL International corporation, cat#312, dilution 1:500), anti-human NG2 (Sigma,
433 cat# MAB2029, 1:200 dilution), anti-vGluT1 (Synaptic system, cat#N1602-AF647-L, 1:500 dilution), and
434 anti-PSD95 (Thermo Fisher, cat#51-6900, 1:500 dilution). After primary antibody incubation, sections
435 were washed three times with PBS and incubated with secondary antibodies at room temperature for 2
436 hours, followed by three additional washes in PBS. Stained sections were mounted onto Superfrost Plus
437 slides (Fisher, cat#12-550-15), covered with mounting medium (Fisher, cat#H1400NB), and sealed with
438 glass coverslips. Fluorescent imaging was carried out on a Zeiss Apotome epifluorescence microscope
439 and a Leica Stellaris confocal microscope with consistent power and exposure settings for all samples
440 processed with the same probe set.

441

442 **RNAscope**

443 Glia-immune humanized mice were transcardially perfused with RNase-free PBS followed by fixation with
444 RNase-free 4% PFA. Brains were removed and post-fixed in 4% PFA for an additional 2 hr at room
445 temperature and then overnight at 4 °C. Brains were dehydrated in RNase-free 30% sucrose, embedded
446 in OCT compound, and cut into 20 μm-thick sections using a Leica cryostat. RNAscope experiments
447 were performed using the RNAscope Multiplex Fluorescent Reagent Kit v2 (ACDBio, cat#323100)
448 according to the manufacturer's protocol. Probes specific to human SLC1A3 (cat#461081-C1), and
449 human CSF1R (cat#310811-C2) were obtained from ACDBio and used for this study. Fluorescent
450 imaging was carried out on a Zeiss Apotome epifluorescence microscope.

451

452 **RNAseq**

453 Total RNA was extracted from humanized mouse brain tissues and prepared for Illumina sequencing
454 following standard protocols. Technical replicate FASTQ files were concatenated, and initial quality
455 assessments were performed using FastQC. Unique molecular identifiers (UMIs) were extracted with
456 UMI-tools, while adapter and low-quality bases were trimmed with Trim Galore!. We then removed
457 genomic contaminants using BBSplit and filtered out rRNA sequences with SortMeRNA. To
458 accommodate reads derived from both mouse and human cells, we constructed a mixed reference by
459 combining Gencode GRCm39 (mouse) and GRCh38 (human) assemblies and annotations, creating a
460 single index for genome alignment. Reads were aligned to this hybrid reference using STAR, followed by
461 transcript quantification in alignment-based mode with Salmon. Aligned reads were sorted and indexed
462 (SAMtools), and UMIs were used for deduplication with UMI-tools, complemented by duplicate marking
463 (picard MarkDuplicates). We then assembled transcripts using StringTie, and coverage tracks (bigWig
464 format) were generated via BEDTools and bedGraphToBigWig. Multiple quality-control checks were
465 performed (RSeQC, Qualimap, dupRadar, and Preseq) to evaluate alignment, duplication rates, and
466 library complexity. Finally, differential expression was assessed using DESeq2, and downstream

467 functional analyses—including Gene Ontology, Reactome pathway enrichment, and additional
468 annotation through clusterProfiler—were conducted in R.
469
470 **Study approval**
471 Peripheral blood mononuclear cells were obtained at UCLA in accordance with UCLA IRB–approved
472 protocols under written informed consent using an IRB-approved written consent form by the UCLA
473 Center for AIDS Research Virology Laboratory and distributed for this study without personal identifying
474 information. Human tissue was obtained from UCLA Pathology Core Laboratory without identifying
475 information and did not require IRB approval for its use. Animal research described in this article was
476 performed under the written approval of the UCLA Animal Research Committee in accordance with all
477 federal, state, and local guidelines. All surgeries were performed under ketamine/xylazine and isoflurane
478 anesthesia, and all efforts were made to minimize animal pain and discomfort.
479
480 **Acknowledgement**
481 We thank UCLA Center for AIDS Research (CFAR) Humanized Mouse Core staff research associate
482 Nianxin Zhong for his assistance in the humanized mice work. This work was funded by the National
483 Institute of Allergy and Infectious Diseases (R01AI172727 to AZ and MDM), the National Institute on
484 Drug Abuse (R01DA052841, R01DA059873 to AZ), National Institute of Health grants P30AI28697 (to
485 the UCLA CFAR Virology Core, Gene and Cell Therapy Core, and Humanized Mouse Core) and
486 U19AI149504 (to SGK and Dr. Irvin Chen [UCLA]); the California Institute for Regenerative Medicine
487 (grant TRAN1-14625 to SGK.); California HIV/AIDS Research Program (grant H24BD7817 to WM);
488 UCLA-Charles Drew University (CDU) CFAR (grant AI152501 to WM); the NIH/NINDS R01NS109025,
489 the Broad Stem Cell Research Center (BSCRC) Innovation Award, the W.M. Keck Foundation Junior
490 Faculty Award, UCLA Jonsson Comprehensive Cancer Center and BSCRC Ablon Scholars Award, Rose
491 Hills Foundation Stem Cell Innovation Award, the BSCRC and California NanoSystems Institute Stem
492 Cell Nano-Medicine Initiative Planning Award, the BSCRC transformative technology development award

493 to Y. Z.; the National Institute of Neurological Disorders and Stroke (R01NS137919 to JW), National
494 Cancer Institute (R01CA253215 to JW). This work was also supported by the UCLA AIDS Institute, the
495 James B. Pendleton Charitable Trust, and the McCarthy Family Foundation. The graphic figure was
496 created with BioRender.com.

497 **Figures and Figure legends**

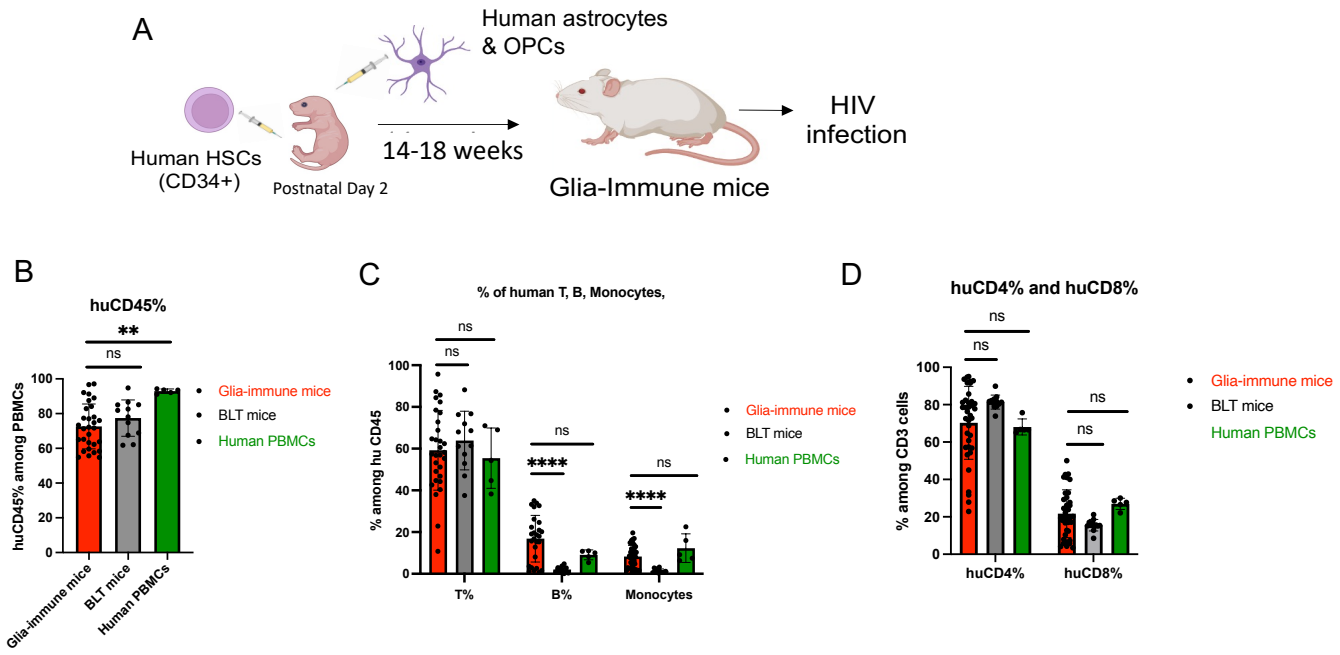

498

499 **Figure 1. Successful engraftment and differentiation of human immune and glial cells in glia-**
500 **immune humanized mice.** A) Human astrocytes and OPCs were transplanted into the subcortical areas
501 of the brains at 1-2mm depth and donor matched human CD34+ HSCs were co-transplanted into the
502 livers of immunodeficient mice at postnatal Day 2. 14-18 weeks after reconstitution, mice were bled and
503 human immune reconstitution was assessed by flow-cytometry by staining with human antibodies. B)
504 Percentage of huCD45+ cells in PBMCs from the glia-immune humanized mice (n=30), humanized BLT
505 mice (n=12) or primary human PBMCs from healthy donors (n=5). C) Percentage of human T cells
506 (huCD3), B cells (huCD19), Monocytes (huCD14) among huCD45 positive cells. D) Percentage of human
507 T-Helper cells (huCD4) and T-cytotoxic cells (huCD8) among T cells. **p=0.0056, ****p<0.0001 by Mann-
508 Whitney test.

509

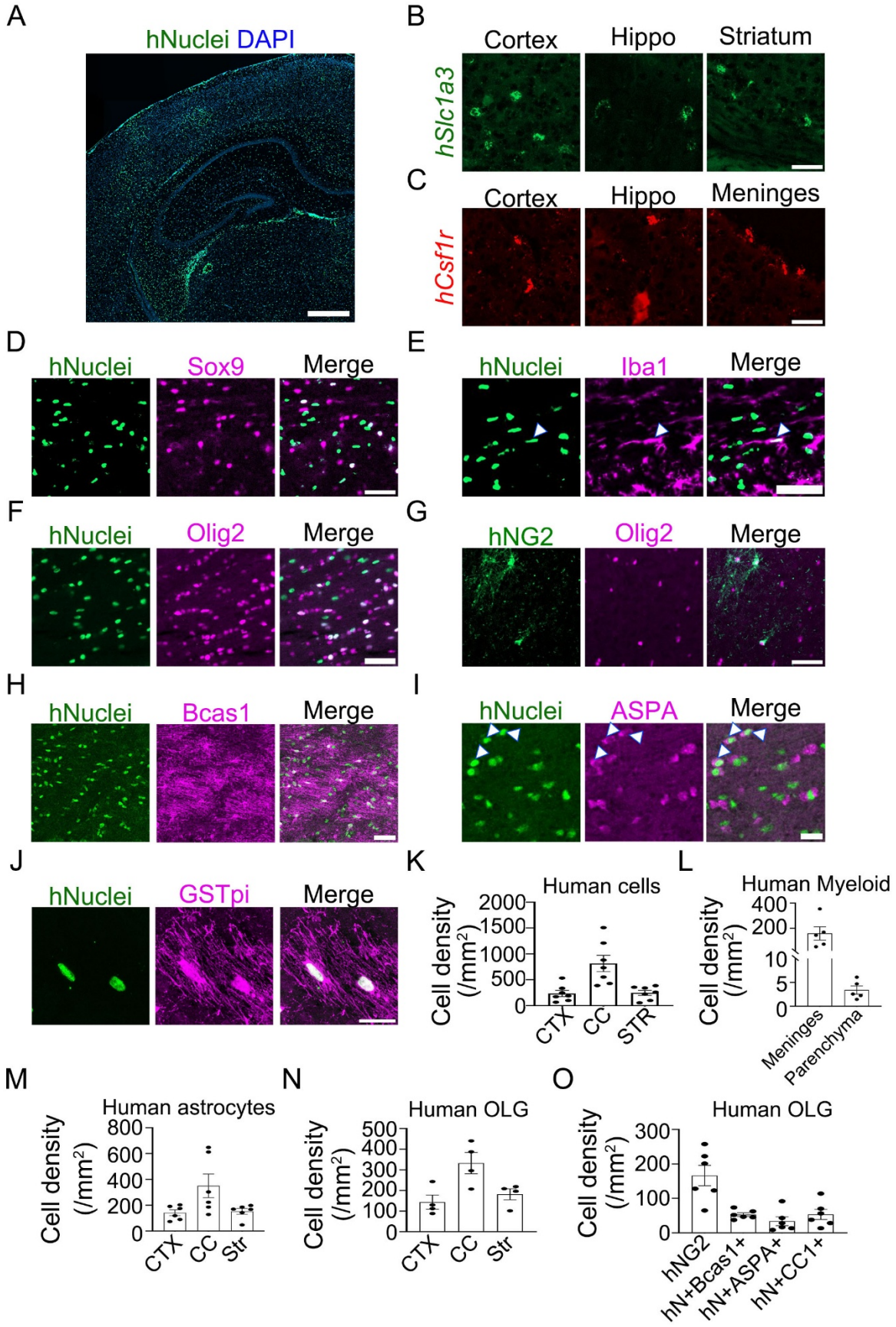
A
hNuclei DAPI
B
Cortex
Hippo
Striatum
hSlc1a3
C
Cortex
Hippo
Meninges
hCsf1r
D
hNuclei
Sox9
Merge
E
hNuclei
Iba1
Merge
F
hNuclei
Olig2
Merge
G
hNG2
Olig2
Merge
H
hNuclei
Bcas1
Merge
I
hNuclei
ASPA
Merge
J
hNuclei
GSTpi
Merge
K
Human cells
Cell density (/mm²)
2000
1500
1000
500
0
CTX
CC
STR
L
Human Myeloid
Cell density (/mm²)
400
200
10
5
0
Meninges
Parenchyma
M
Human astrocytes
Cell density (/mm²)
800
600
400
200
0
CTX
CC
Str
N
Human OLG
Cell density (/mm²)
500
400
300
200
100
0
CTX
CC
Str
O
Human OLG
Cell density (/mm²)
300
200
100
0
hNG2
hN+Bcas1+
hN+ASPA+
hN+CC1+

510

511 **Figure 2. Widespread engraftment of human glia (astrocytes, OPCs, oligodendrocytes, and**
512 **microglia-like cells) in the brains of glia-immune humanized mice.** A) Human nuclei staining reveals
513 widespread distribution of human cells in the chimeric mouse brain. Scale bar: 500 μm. Green: human
514 nuclei. Blue: DAPI. B) *hSlc1a3* RNAscope assay demonstrates the presence of human astrocytes in the
515 cortex, hippocampus, and striatum of the chimeric mouse brain. Scale bar: 50 μm. C) *hCsf1r* RNAscope
516 assay shows human microglia-like cells in the cortex, hippocampus (hippo), and meninges of the chimeric
517 mouse brain. Scale bar: 50 μm. D) Colocalization of human nuclei with astrocyte marker Sox9 indicates
518 the presence of human astrocytes in the chimeric mouse brain. Scale bar: 50 μm. E) Colocalization of
519 human nuclei with microglia-like cell marker Iba1 indicates the presence of human microglia-like cells
520 (arrowheads) in the chimeric mouse brain. Scale bar: 50 μm. F) Colocalization of human nuclei with
521 oligodendroglial marker Olig2 indicates the presence of Oligodendroglia in the chimeric mouse brain.
522 Scale bar: 20 μm. G) Immunostaining of human NG2 shows the presence of human OPCs in the chimeric
523 mouse brain. Scale bar: 50 μm. H) Colocalization of human nuclei with newly differentiated
524 premyelinating oligodendrocyte marker Bcas1 indicates the presence of human immature
525 oligodendrocytes in the chimeric mouse brain. Scale bar: 20 μm. I) Colocalization of human nuclei with
526 mature oligodendrocyte marker ASPA indicates the presence of human mature oligodendrocytes in the
527 chimeric mouse brain. Scale bar: 20 μm. J) Colocalization of human nuclear marker with the mature
528 oligodendrocyte marker GSTpi confirms the presence of human oligodendrocytes with mature,
529 myelinating morphology in the chimeric mouse brain. Scale bar: 20 μm. K) Quantification of the densities
530 of human cells (human nuclei+ cells) in the cortex (CTX), corpus callosum (CC), and striatum (STR) (n=
531 7). L) Quantification of the densities of human meningeal myeloid cells (human *Csf1r*+ cells) and human
532 microglia-like cells (human *Csf1r*+ cells) in the brain parenchyma of the chimeric mouse brain (n = 6). M)
533 Quantification of the densities of human astrocytes (human nuclei+, Sox9+ double-positive cells) in the
534 cortex, corpus callosum, hippocampus, and thalamus (Tha) of the chimeric mouse brain (n = 6). N)
535 Quantification of the densities of human oligodendroglia cells (human nuclei+, Olig2+ double-positive
536 cells) in the CTX, CC and Stratum (n = 4). O) Quantification of the densities of human OPCs (human

537 NG2+ cells), human immature oligodendrocytes (human nuclei+, Bcas1+ double-positive cells), human
538 mature oligodendrocytes (human nuclei+, ASPA+ double-positive cells), and human differentiated
539 oligodendrocytes (human nuclei+, CC1+ double-positive cells) in the corpus callosum (n = 6).
540

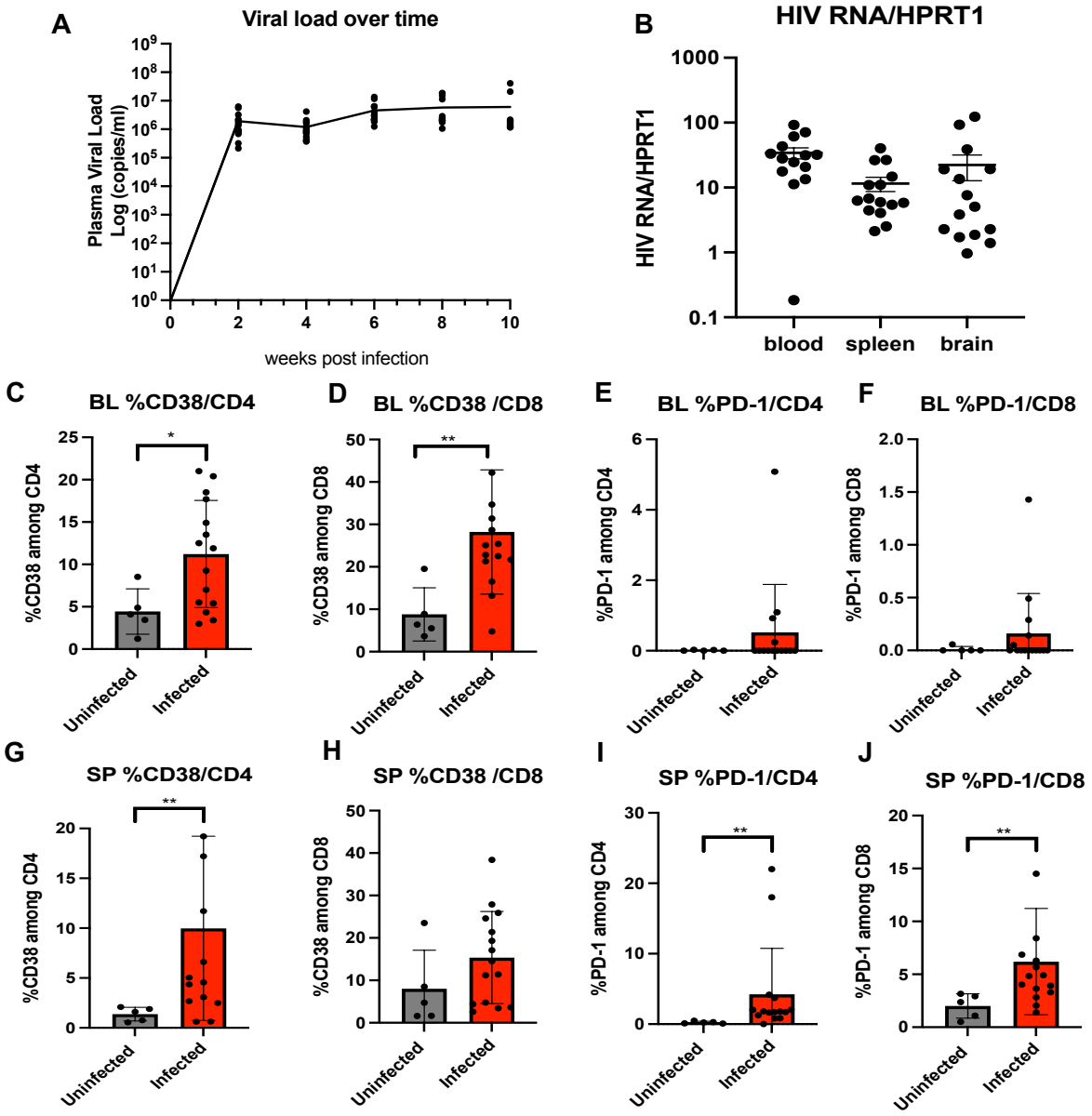

Figure 3. HIV infection and elevated Immune activation/exhaustion in infected glia-immune humanized mice. Glia-immune humanized mice were infected with HIV-1 CH040 (n=15) or mock infected (n=5) to evaluate viral replication and immune dysregulation. A) Plasma viral load was quantified longitudinally by real-time PCR. The X-axis represents time (in weeks) and the y-axis shows the plasma viral load in copies/ml (log scale). B) 10 weeks after HIV infection, mice were sacrificed, perfused with PBS and tissues were harvested. Viral RNA in blood, spleen and brain was quantified by real-time PCR.

549 HPRT1 is internal control for normalization of gene expression. Data are presented as Mean± SEM. C-
550 J) PBMCs from Blood (BL) and Splenocytes from spleen (SP) at week 10 were processed and stained
551 for activation (CD38) (C, D, E, F) and exhaustion markers (PD-1) (G, H, I, J) on $CD4^+$ and $CD8^+$ T-cells
552 using Flow-cytometry. Percentage of cells positive for each marker is represented as Mean ± S.D. *
553 p=0.0328, **p=0.0037 in BL %CD38/CD8, **p=0.0077 in SP %CD38/CD4, **p=0.0024 in SP %PD-1/CD4,
554 **p=0.0077 in SP %PD-1/CD8 by Mann-Whitney test.

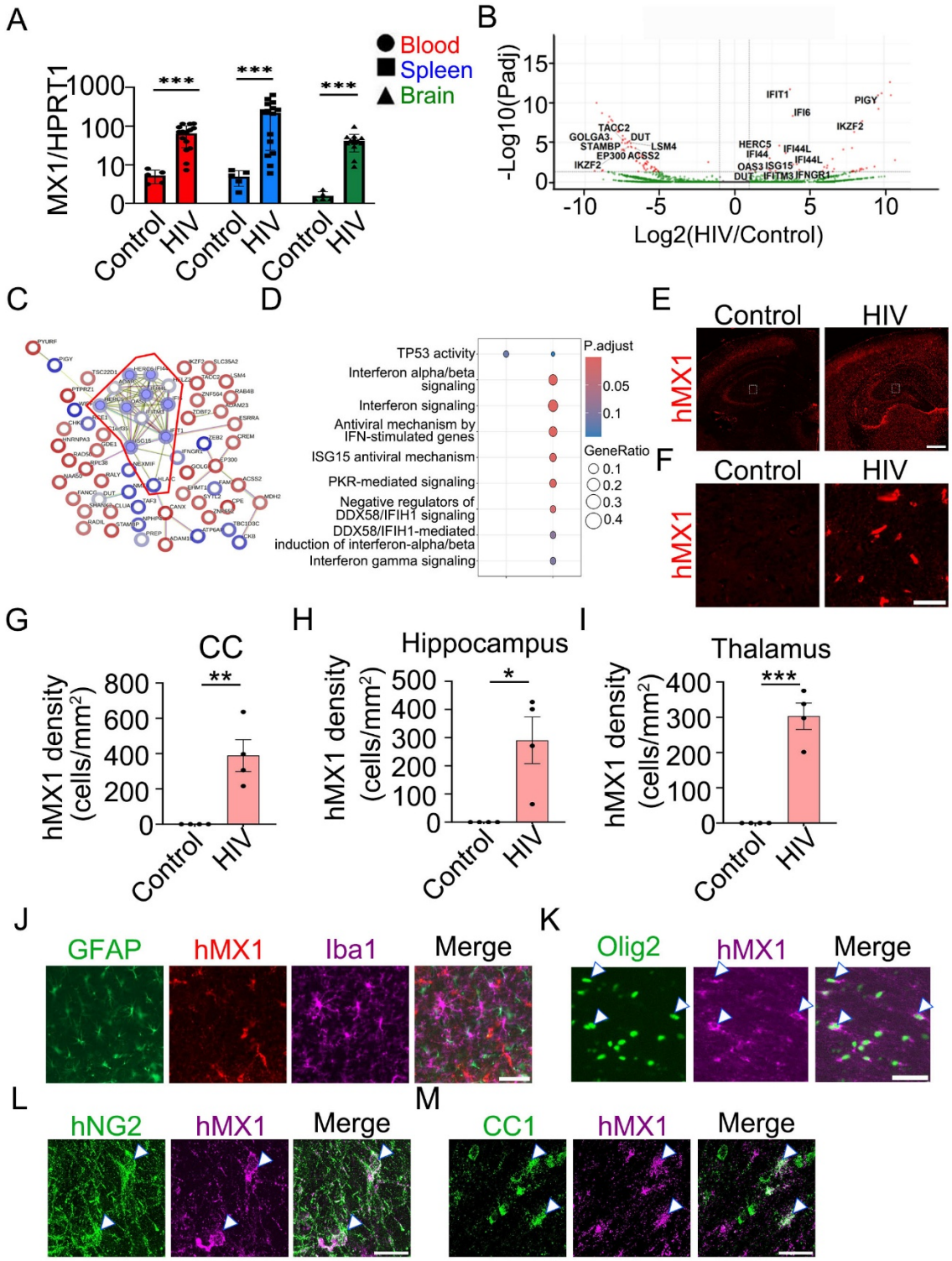

Figure 4: HIV infection induces upregulation of human-specific interferon response gene MX1 in glia-immune humanized mice. A) Interferon stimulated gene -MX1 expression level in blood, spleen and brain as measured by real-time PCR in uninfected (n=5) and infected mice (n=15). HPRT1 is

internal control for normalization of gene expression. B) Volcano plot showing differential gene expression of infected versus uninfected brains. The x-axis represents the $\log_2$ fold change ($\log_2$FC) in gene expression while the y-axis shows the $-\log_{10}$ p-value. Genes with significant differential expression are highlighted in red. C) Reactome pathway analysis of significantly differentially expressed genes in the brains of infected versus uninfected mice**.** This network visualization displays the interactions between genes with significant changes in expression. Nodes represent individual genes, and edges indicate known or predicted interactions based on pathway data. The network shows a highly interconnected cluster of genes, including ISG15 and OAS1 involved in interferon signaling pathways and the antiviral response. D) Gene enrichment analysis. Red circle highlights genes involved in interferon signaling. E) Human MX1 (hMX1) staining shows a widespread upregulation of the interferon response in the brains of glia-immune humanized mice following HIV infection (n=4). Scale bar: 500 μm. Zoomed in images (dashed rectangular area in F) shows increased human MX1+ cells in the hippocampus of the glia-immune humanized mouse. (G-I). Quantification of the densities of human MX1+ cells in the corpus callosum (CC), cortex, hippocampus, and thalamus of the chimeric mouse brain. (*p=0.0127 by unpaired t-test in Hippocampus, **p=0.0051 by unpaired t-test in CC, ***p=0.0002 by unpaired t-test in Thalamus, ***p=0.0003 in blood, ***p=0.0005 in spleen, **p=0.0001 in brain by Mann-Whitney test.) J) Limited colocalization of hMX1 (red) with astrocyte (GFAP+ green) or microglia (Iba1+ purple). K) Colocalization (yellow) of hMX1 (red) with Oligodendroglia (Olig2+ in green). L) Colocalization (white) of hMX1 (purple) with human oligodendroglia precursor cells (hNG2+ in green). Scale bar: 20 μm. M) Colocalization (white) of hMX1 (purple) with differentiated oligodendroglia marker (CC1+ in green). Scale bar: 20 μm.

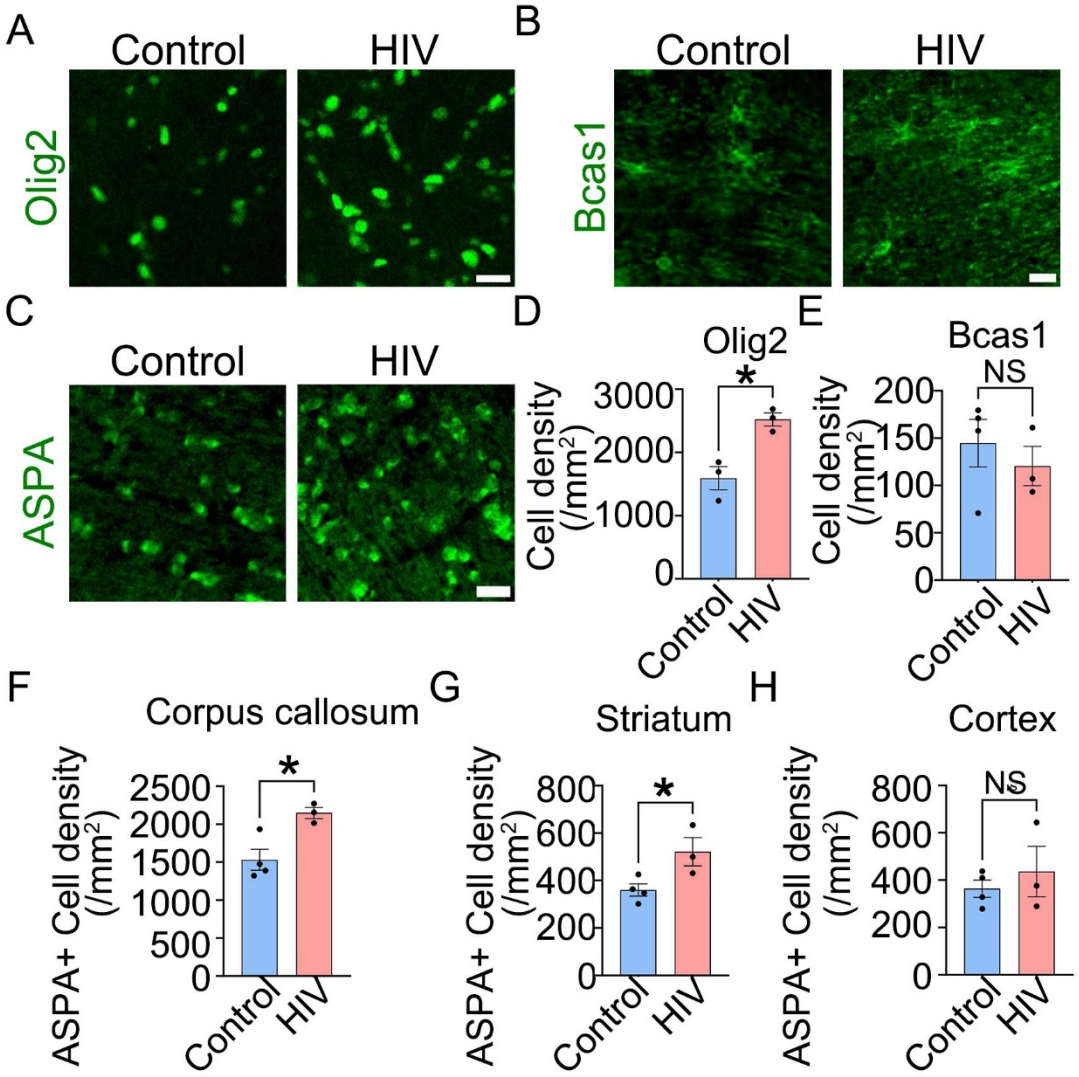

Figure 5. HIV infection increases the densities of oligodendrocytes in glia-immune humanized mice. A) Immunostaining of Olig2 shows an increase in the number of oligodendroglia (olig2+ cells) after HIV infection. Scale bar: 20 μm. B) Immunostaining of Bcas1 shows no change in the number of immature oligodendrocytes (Bcas1+ cells) after HIV infection. Scale bar: 20 μm. C) Immunostaining of ASPA shows an increase in the number of mature oligodendrocytes (ASPA+ cells) after HIV infection. Scale bar: 20 μm. D) Quantification of the densities of oligodendroglia (Olig2+ cells) in the corpus callosum of the chimeric mouse brain. (n = 3, p = 0.0117 by unpaired t-test.) E) Quantification of the densities of immature oligodendrocytes (Bcas1+ cells) in the corpus callosum of the chimeric mouse brain. (n = 4 for Control, n = 3 for HIV, p = 0.5128, unpaired t-test). F to H) Quantification of the

595 densities of mature oligodendrocytes (ASPA+ cells) in the corpus callosum, striatum, and cortex of the
596 chimeric mouse brain. (n = 4 for Control, n = 3 for HIV, p = 0.0169 for CC, p = 0.0395 for STR, p =
597 0.4962 for CTX, unpaired t-test).
598
599

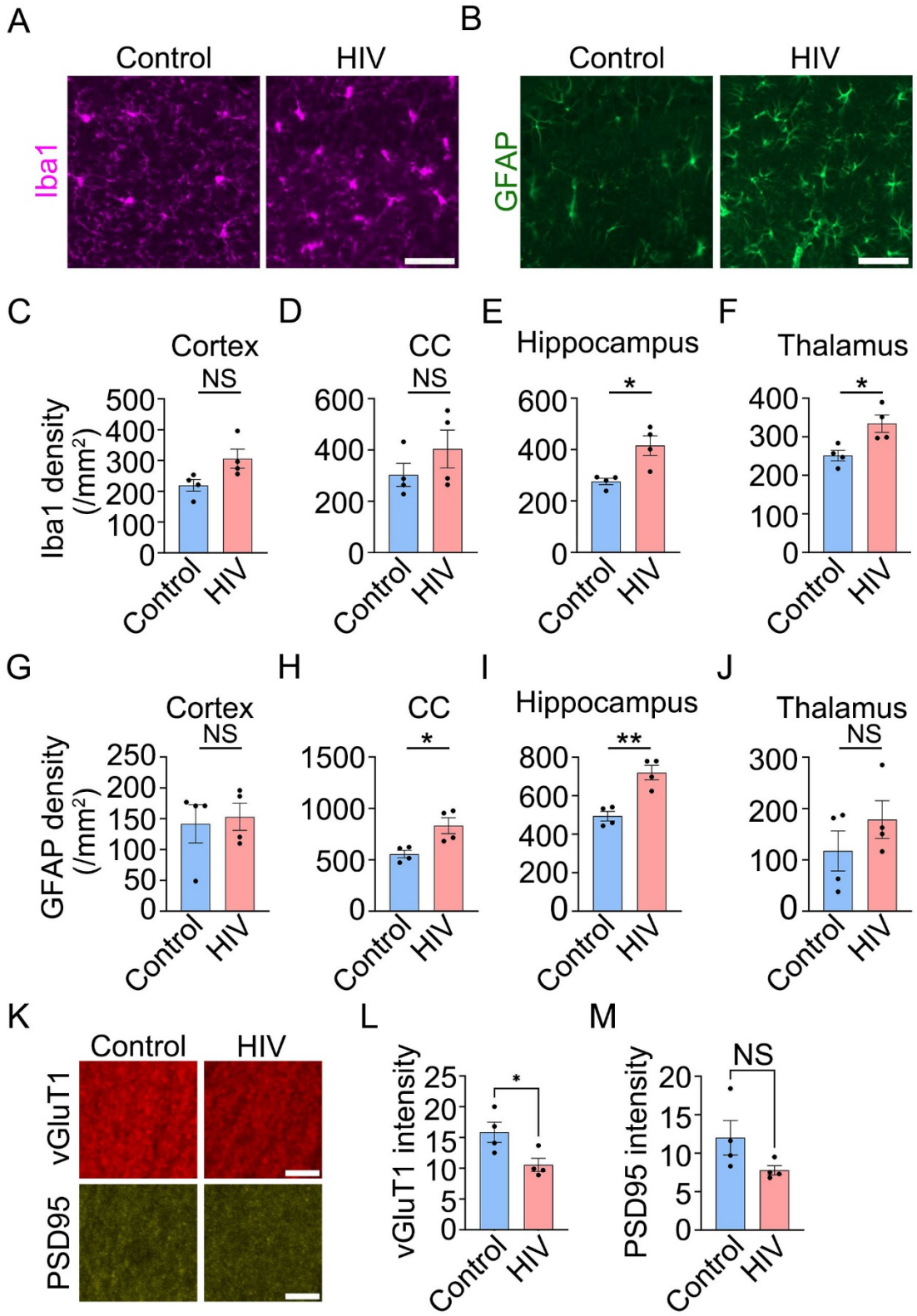

Figure 6. HIV infection leads to microglia, astrocyte reactivity and loss of synaptic proteins in the chimeric mouse brain. A) Iba1 staining in the hippocampus shows that microglia density is increased

603 after HIV infection. Scale bar: 50 μm. B) GFAP staining in the hippocampus shows that GFAP+ astrocytes
604 density is increased after HIV infection. Scale bar: 50 μm. (C - F) Quantification of the density of Iba1+
605 cells in the cortex, corpus callosum, hippocampus, and thalamus of the chimeric mouse brain. ($n = 4$, p
606 $= 0.0553$ for CTX, $p = 0.288$ for CC, $p = 0.0131$ for Hippo, $p = 0.0197$ for thalamus). (G - J) Quantification
607 of the density of GFAP+ cells in the cortex, corpus callosum, hippocampus, and thalamus of the chimeric
608 mouse brain. ($n = 4$, $p = 0.7771$ for CTX, $p = 0.0182$ for CC, $p = 0.0024$ for Hippo, $p = 0.2966$ for thalamus).
609 (*$p<0.05$, **$p<0.005$, by unpaired t-test). (*$p<0.05$, **$p<0.005$, by unpaired t-test). K) vGluT1 and PSD95
610 staining in the CA1 region of hippocampus shows a decrease in vGluT1 immunofluorescence intensity
611 after HIV infection and no change in PSD95 immunofluorescence intensity. Scale bar: 5 μm. L)
612 Quantification of the intensity of vGluT1 in the CA1 region of hippocampus from the chimeric mouse brain.
613 ($n = 4$, $p = 0.0355$). M) Quantification of the intensity of PSD95 in the CA1 region of hippocampus from
614 the chimeric mouse brain. ($n = 4$, $p = 0.1178$ for CTX).
615

616

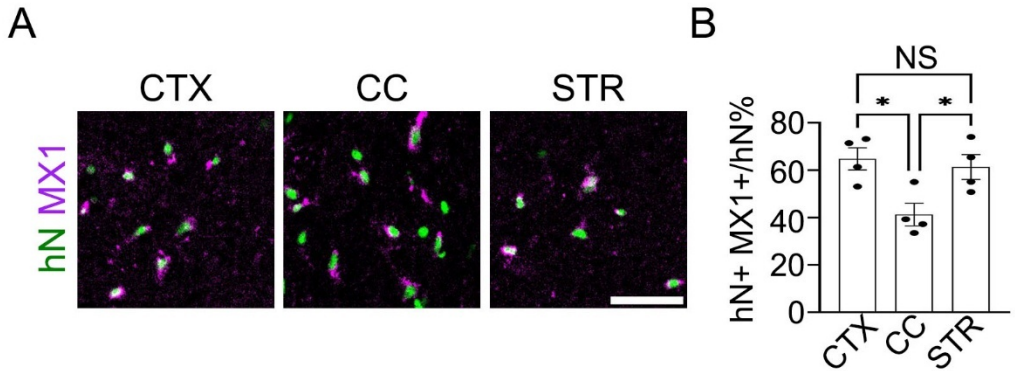

617

618 **Supplementary Fig. 1. Regional heterogeneity in the adoption of immune oligodendroglia state.**
619 (A) Human nuclei (hN) and human MX1 double-staining in cortex (CTX), corpus callosum (CC), and
620 striatum (STR) shows that a smaller proportion of human cells in the CC adopt an immune
621 oligodendroglial state compared to CTX and STR. Scale bar: 50 μm. (B) Quantification of the percentage
622 of hN^+ cells expressing MX1 in different brain regions (n = 4). One-way ANOVA with Tukey's multiple
623 comparison correction: CTX vs CC, p = 0.0244; CC vs STR, p = 0.0207; CTX vs STR, p = 0.6147.

624

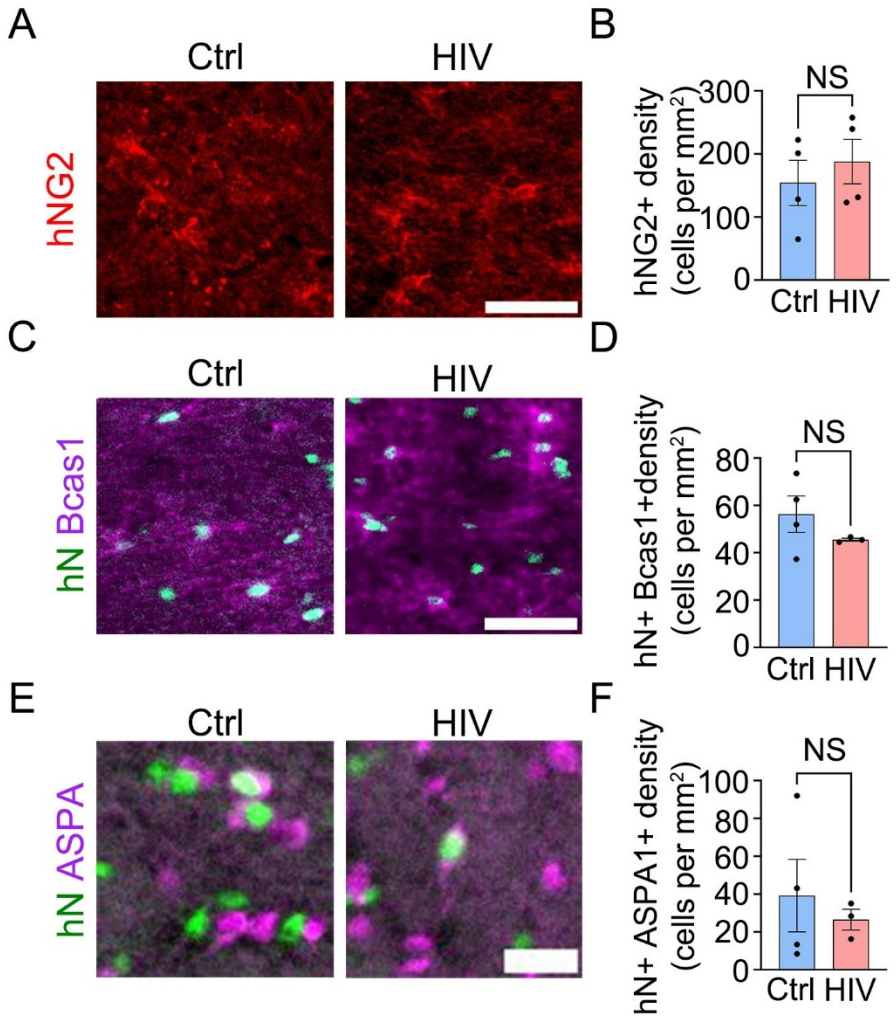

625

626 **Supplementary Fig. 2. HIV infection does not alter the densities of human oligodendroglia in the**
627 **chimeric mouse brain.** (A) Immunostaining for human NG2 in the corpus callosum shows no change in
628 the densities of human oligodendrocyte precursor cells after HIV infection. Scale bar: 50 μm. (B)
629 Quantification of $hNG2^+$ cell density in the corpus callosum (Ctrl: n = 4; HIV: n = 4; unpaired t test, p =
630 0.5263). (C) Human nuclei (hN) and Bcas1 double-staining shows no change in immature human
631 oligodendrocyte (hN^+Bcas1^+) density after HIV infection. Scale bar: 50 μm. (D) Quantification of
632 hN^+Bcas1^+ cell density (Ctrl: n = 4; HIV: n = 3; unpaired t test, p = 0.2914). (E) Human nuclei and ASPA
633 double-staining shows no change in mature human oligodendrocyte (hN^+ASPA^+) density after HIV
634 infection. Scale bar: 20 μm. (F) Quantification of hN^+ASPA^+ cell density (Ctrl: n = 4; HIV: n = 3; unpaired
635 t test, p = 0.6085).

636 **References**

637

638 1 Adamu, A., Li, S., Gao, F. & Xue, G. The role of neuroinflammation in neurodegenerative diseases:
639 current understanding and future therapeutic targets. *Front Aging Neurosci* **16**, 1347987 (2024).
640 https://doi.org/10.3389/fnagi.2024.1347987
641 2 Zhang, W., Xiao, D., Mao, Q. & Xia, H. Role of neuroinflammation in neurodegeneration
642 development. *Signal Transduct Target Ther* **8**, 267 (2023). https://doi.org/10.1038/s41392-023-
643 01486-5
644 3 Li, J. *et al.* Conservation and divergence of vulnerability and responses to stressors between human
645 and mouse astrocytes. *Nat Commun* **12**, 3958 (2021). https://doi.org/10.1038/s41467-021-24232-
646 3
647 4 Goldman, S. A. Glial evolution as a determinant of human behavior and its disorders. *Ann N Y*
648 *Acad Sci* **1471**, 72-85 (2020). https://doi.org/10.1111/nyas.14372
649 5 Summers, R. A., Fagiani, F., Rowitch, D. H., Absinta, M. & Reich, D. S. Novel human iPSC
650 models of neuroinflammation in neurodegenerative disease and regenerative medicine. *Trends*
651 *Immunol* **45**, 799-813 (2024). https://doi.org/10.1016/j.it.2024.08.004
652 6 Preman, P. *et al.* Human iPSC-derived astrocytes transplanted into the mouse brain undergo
653 morphological changes in response to amyloid-beta plaques. *Mol Neurodegener* **16**, 68 (2021).
654 https://doi.org/10.1186/s13024-021-00487-8
655 7 Carrillo, M. A., Zhen, A. & Kitchen, S. G. The Use of the Humanized Mouse Model in Gene
656 Therapy and Immunotherapy for HIV and Cancer. *Front Immunol* **9**, 746 (2018).
657 https://doi.org/10.3389/fimmu.2018.00746
658 8 Marsden, M. D. & Zack, J. A. Humanized Mouse Models for Human Immunodeficiency Virus
659 Infection. *Annu Rev Virol* **4**, 393-412 (2017). https://doi.org/10.1146/annurev-virology-101416-
660 041703
661 9 Wahl, A. & Garcia, J. V. Humanized Mouse Systems to Study Viral Infection: A New Era in
662 Immunology Research. *Annu Rev Immunol* **43**, 143-167 (2025). https://doi.org/10.1146/annurev-
663 immunol-082223-035718
664 10 Wang, Y. *et al.* Global prevalence and burden of HIV-associated neurocognitive disorder: A meta-
665 analysis. *Neurology* **95**, e2610-e2621 (2020). https://doi.org/10.1212/WNL.0000000000010752
666 11 Borrajo, A., Spuch, C., Penedo, M. A., Olivares, J. M. & Agis-Balboa, R. C. Important role of
667 microglia in HIV-1 associated neurocognitive disorders and the molecular pathways implicated in
668 its pathogenesis. *Ann Med* **53**, 43-69 (2021). https://doi.org/10.1080/07853890.2020.1814962
669 12 Valdebenito, S., Castellano, P., Ajasin, D. & Eugenin, E. A. Astrocytes are HIV reservoirs in the
670 brain: A cell type with poor HIV infectivity and replication but efficient cell-to-cell viral transfer.
671 *J Neurochem* **158**, 429-443 (2021). https://doi.org/10.1111/jnc.15336
672 13 Jensen, B. K., Roth, L. M., Grinspan, J. B. & Jordan-Sciutto, K. L. White matter loss and
673 oligodendrocyte dysfunction in HIV: A consequence of the infection, the antiretroviral therapy or
674 both? *Brain Res* **1724**, 146397 (2019). https://doi.org/10.1016/j.brainres.2019.146397
675 14 Roth, L. M., Akay-Espinoza, C., Grinspan, J. B. & Jordan-Sciutto, K. L. HIV-induced
676 neuroinflammation inhibits oligodendrocyte maturation via glutamate-dependent activation of the
677 PERK arm of the integrated stress response. *Glia* **69**, 2252-2271 (2021).
678 https://doi.org/10.1002/glia.24033
679 15 Liu, H., Xu, E., Liu, J. & Xiong, H. Oligodendrocyte Injury and Pathogenesis of HIV-1-Associated
680 Neurocognitive Disorders. *Brain Sci* **6** (2016). https://doi.org/10.3390/brainsci6030023

16 Veazey, R. S. & Lackner, A. A. Nonhuman Primate Models and Understanding the Pathogenesis of HIV Infection and AIDS. *ILAR J* **58**, 160-171 (2017). https://doi.org/10.1093/ilar/ilx032

17 Zhen, A. *et al.* Robust CAR-T memory formation and function via hematopoietic stem cell delivery. *PLoS Pathog* **17**, e1009404 (2021). https://doi.org/10.1371/journal.ppat.1009404

18 Zhen, A. *et al.* HIV-specific Immunity Derived From Chimeric Antigen Receptor-engineered Stem Cells. *Molecular therapy : the journal of the American Society of Gene Therapy* **23**, 1358-1367 (2015). https://doi.org/10.1038/mt.2015.102

19 Norton, T. D. *et al.* Lentiviral Vector-Based Dendritic Cell Vaccine Suppresses HIV Replication in Humanized Mice. *Molecular therapy : the journal of the American Society of Gene Therapy* **27**, 960-973 (2019). https://doi.org/10.1016/j.ymthe.2019.03.008

20 Maldini, C. R. *et al.* Dual CD4-based CAR T cells with distinct costimulatory domains mitigate HIV pathogenesis in vivo. *Nature medicine* **26**, 1776-1787 (2020). https://doi.org/10.1038/s41591-020-1039-5

21 Marsden, M. D. *et al.* Tracking HIV Rebound following Latency Reversal Using Barcoded HIV. *Cell Rep Med* **1**, 100162 (2020). https://doi.org/10.1016/j.xcrm.2020.100162

22 Marsden, M. D. *et al.* In vivo activation of latent HIV with a synthetic bryostatin analog effects both latent cell "kick" and "kill" in strategy for virus eradication. *PLoS pathogens* **13**, e1006575 (2017). https://doi.org/10.1371/journal.ppat.1006575

23 Carrillo, M. A. *et al.* Stem cell-derived CAR T cells show greater persistence, trafficking, and viral control compared to ex vivo transduced CAR T cells. *Mol Ther* **32**, 1000-1015 (2024). https://doi.org/10.1016/j.ymthe.2024.02.026

24 Mu, W., Patankar, V., Kitchen, S. & Zhen, A. Examining Chronic Inflammation, Immune Metabolism, and T Cell Dysfunction in HIV Infection. *Viruses* **16** (2024). https://doi.org/10.3390/v16020219

25 Mu, W. *et al.* Autophagy inducer rapamycin treatment reduces IFN-I-mediated Inflammation and improves anti-HIV-1 T cell response in vivo. *JCI Insight* **7** (2022). https://doi.org/10.1172/jci.insight.159136

26 Mu, W. *et al.* Oral Combinational Antiretroviral Treatment in HIV-1 Infected Humanized Mice. *J Vis Exp* (2022). https://doi.org/10.3791/63696

27 Zhen, A. *et al.* Targeting type I interferon-mediated activation restores immune function in chronic HIV infection. *J Clin Invest* **127**, 260-268 (2017). https://doi.org/10.1172/JCI89488

28 Zhen, A. *et al.* Stem-cell Based Engineered Immunity Against HIV Infection in the Humanized Mouse Model. *Journal of visualized experiments : JoVE* (2016). https://doi.org/10.3791/54048

29 Victor Garcia, J. Humanized mice for HIV and AIDS research. *Current opinion in virology* **19**, 56-64 (2016). https://doi.org/10.1016/j.coviro.2016.06.010

30 Marsden, M. D. Benefits and limitations of humanized mice in HIV persistence studies. *Retrovirology* **17**, 7 (2020). https://doi.org/10.1186/s12977-020-00516-2

31 Rogers, G. L. *et al.* Reprogramming human B cells with custom heavy-chain antibodies. *Nat Biomed Eng* (2024). https://doi.org/10.1038/s41551-024-01240-4

32 Hofer, U. *et al.* Pre-clinical modeling of CCR5 knockout in human hematopoietic stem cells by zinc finger nucleases using humanized mice. *The Journal of infectious diseases* **208 Suppl 2**, S160-164 (2013). https://doi.org/10.1093/infdis/jit382

33 Mu, W. a. R., Valerie and Martin, Heather and Carrillo, Mayra and Hamid, Philip and Lizarraga, Miguel and Yang, Otto O. and Jamieson, Beth and Kitchen, Scott G. and Zhen, Anjie. . Induction of Autophagy Reduces IFN-I Mediated Inflammation and Restores Anti-HIV-1 T Cell Response in vivo. *Cell Reports Sneak Peek* (2021). https://doi.org/http://dx.doi.org/10.2139/ssrn.3895931

727 34 Lutgen, V. *et al.* HIV infects astrocytes in vivo and egresses from the brain to the periphery. *PLoS*
728 *pathogens* **16**, e1008381 (2020). https://doi.org/10.1371/journal.ppat.1008381
729 35 Zhang, J. *et al.* Human Microglia Extensively Reconstitute in Humanized-BLT Mice With Human
730 Interleukin-34 Transgene and Support HIV-1 Brain Infection. *Frontiers in immunology* **12**, 672415
731 (2021). https://doi.org/10.3389/fimmu.2021.672415
732 36 Mathews, S. *et al.* Human Interleukin-34 facilitates microglia-like cell differentiation and
733 persistent HIV-1 infection in humanized mice. *Mol Neurodegener* **14**, 12 (2019).
734 https://doi.org/10.1186/s13024-019-0311-y
735 37 Waight, E. *et al.* Animal models for studies of HIV-1 brain reservoirs. *Journal of leukocyte biology*
736 **112**, 1285-1295 (2022). https://doi.org/10.1002/JLB.5VMR0322-161R
737 38 Chien, A. *et al.* White and Gray Matter Changes are Associated With Neurocognitive Decline in
738 HIV Infection. *Ann Neurol* **95**, 941-950 (2024). https://doi.org/10.1002/ana.26896
739 39 Yang, J. *et al.* Multi-omic Characterization of HIV Effects at Single Cell Level across Human
740 Brain Regions. *bioRxiv* (2025). https://doi.org/10.1101/2025.02.05.636707
741 40 Jaeger, L. B. & Nath, A. Modeling HIV-associated neurocognitive disorders in mice: new
742 approaches in the changing face of HIV neuropathogenesis. *Dis Model Mech* **5**, 313-322 (2012).
743 https://doi.org/10.1242/dmm.008763
744 41 Price, T. O., Ercal, N., Nakaoke, R. & Banks, W. A. HIV-1 viral proteins gp120 and Tat induce
745 oxidative stress in brain endothelial cells. *Brain Res* **1045**, 57-63 (2005).
746 https://doi.org/10.1016/j.brainres.2005.03.031
747 42 Hong, S. & Banks, W. A. Role of the immune system in HIV-associated neuroinflammation and
748 neurocognitive implications. *Brain Behav Immun* **45**, 1-12 (2015).
749 https://doi.org/10.1016/j.bbi.2014.10.008
750 43 Shimizu, S. *et al.* RNAi-Mediated CCR5 Knockdown Provides HIV-1 Resistance to Memory T
751 Cells in Humanized BLT Mice. *Molecular therapy. Nucleic acids* **4**, e227 (2015).
752 https://doi.org/10.1038/mtna.2015.3
753 44 Yi, G. *et al.* CCR5 Gene Editing of Resting CD4(+) T Cells by Transient ZFN Expression From
754 HIV Envelope Pseudotyped Nonintegrating Lentivirus Confers HIV-1 Resistance in Humanized
755 Mice. *Molecular therapy. Nucleic acids* **3**, e198 (2014). https://doi.org/10.1038/mtna.2014.52
756 45 Anthony-Gonda, K. *et al.* Multispecific anti-HIV duoCAR-T cells display broad in vitro antiviral
757 activity and potent in vivo elimination of HIV-infected cells in a humanized mouse model. *Science*
758 *translational medicine* **11** (2019). https://doi.org/10.1126/scitranslmed.aav5685
759 46 Daharsh, L., Zhang, J., Ramer-Tait, A. & Li, Q. A Double Humanized BLT-mice Model Featuring
760 a Stable Human-Like Gut Microbiome and Human Immune System. *Journal of visualized*
761 *experiments : JoVE* (2019). https://doi.org/10.3791/59773
762 47 Claiborne, D. T. *et al.* Immunization of BLT Humanized Mice Redirects T Cell Responses to Gag
763 and Reduces Acute HIV-1 Viremia. *Journal of virology* **93** (2019).
764 https://doi.org/10.1128/JVI.00814-19
765 48 Lavender, K. J. *et al.* An advanced BLT-humanized mouse model for extended HIV-1 cure studies.
766 *AIDS (London, England)* **32**, 1-10 (2018). https://doi.org/10.1097/QAD.0000000000001674
767 49 Karpel, M. E., Boutwell, C. L. & Allen, T. M. BLT humanized mice as a small animal model of
768 HIV infection. *Current opinion in virology* **13**, 75-80 (2015).
769 https://doi.org/10.1016/j.coviro.2015.05.002
770 50 Wahl, A. & Victor Garcia, J. The use of BLT humanized mice to investigate the immune
771 reconstitution of the gastrointestinal tract. *J Immunol Methods* **410**, 28-33 (2014).
772 https://doi.org/10.1016/j.jim.2014.06.009

51 Seung, E. *et al.* PD-1 blockade in chronically HIV-1-infected humanized mice suppresses viral loads. *PloS one* **8**, e77780 (2013). https://doi.org/10.1371/journal.pone.0077780

52 Dudek, T. E. & Allen, T. M. HIV-specific CD8(+) T-cell immunity in humanized bone marrow-liver-thymus mice. *The Journal of infectious diseases* **208 Suppl 2**, S150-154 (2013). https://doi.org/10.1093/infdis/jit320

53 Ringpis, G. E. *et al.* Engineering HIV-1-resistant T-cells from short-hairpin RNA-expressing hematopoietic stem/progenitor cells in humanized BLT mice. *PloS one* **7**, e53492 (2012). https://doi.org/10.1371/journal.pone.0053492

54 Vatakis, D. N. *et al.* Using the BLT humanized mouse as a stem cell based gene therapy tumor model. *Journal of visualized experiments : JoVE*, e4181 (2012). https://doi.org/10.3791/4181

55 Marsden, M. D. *et al.* HIV latency in the humanized BLT mouse. *Journal of virology* **86**, 339-347 (2012). https://doi.org/10.1128/JVI.06366-11

56 Denton, P. W. *et al.* Generation of HIV latency in humanized BLT mice. *Journal of virology* **86**, 630-634 (2012). https://doi.org/10.1128/JVI.06120-11

57 Garcia-Beltran, W. F. *et al.* Innate Immune Reconstitution in Humanized Bone Marrow-Liver-Thymus (HuBLT) Mice Governs Adaptive Cellular Immune Function and Responses to HIV-1 Infection. *Frontiers in immunology* **12**, 667393 (2021). https://doi.org/10.3389/fimmu.2021.667393

58 Yan, H., Semple, K. M., Gonzalez, C. M. & Howard, K. E. Bone marrow-liver-thymus (BLT) immune humanized mice as a model to predict cytokine release syndrome. *Transl Res* **210**, 43-56 (2019). https://doi.org/10.1016/j.trsl.2019.04.007

59 Crawford, L. B. *et al.* Human Cytomegalovirus Induces Cellular and Humoral Virus-specific Immune Responses in Humanized BLT Mice. *Scientific reports* **7**, 937 (2017). https://doi.org/10.1038/s41598-017-01051-5

60 Ginwala, R. *et al.* HTLV-1 Infection and Neuropathogenesis in the Context of Rag1(-/-)gammac(-/-) (RAG1-Hu) and BLT Mice. *Journal of neuroimmune pharmacology : the official journal of the Society on NeuroImmune Pharmacology* **12**, 504-520 (2017). https://doi.org/10.1007/s11481-017-9740-y

61 Cheng, L. *et al.* Blocking type I interferon signaling enhances T cell recovery and reduces HIV-1 reservoirs. *The Journal of clinical investigation* **127**, 269-279 (2017). https://doi.org/10.1172/JCI90745

62 Honeycutt, J. B. *et al.* T cells establish and maintain CNS viral infection in HIV-infected humanized mice. *The Journal of clinical investigation* **128**, 2862-2876 (2018). https://doi.org/10.1172/JCI98968

63 Deeks, S. G., Tracy, R. & Douek, D. C. Systemic effects of inflammation on health during chronic HIV infection. *Immunity* **39**, 633-645 (2013). https://doi.org/10.1016/j.immuni.2013.10.001

64 Mu, W., Kedia, N. & Zhen, A. Finetuning Type I Interferon Signaling to Enhance T Cell Immunity in HIV Infection. *Viruses* **17** (2025). https://doi.org/10.3390/v17060774

65 Soper, A. *et al.* Type I Interferon Responses by HIV-1 Infection: Association with Disease Progression and Control. *Front Immunol* **8**, 1823 (2017). https://doi.org/10.3389/fimmu.2017.01823

66 Wang, B., Kang, W., Zuo, J., Kang, W. & Sun, Y. The Significance of Type-I Interferons in the Pathogenesis and Therapy of Human Immunodeficiency Virus 1 Infection. *Front Immunol* **8**, 1431 (2017). https://doi.org/10.3389/fimmu.2017.01431

67 Thaney, V. E. & Kaul, M. Type I Interferons in NeuroHIV. *Viral Immunol* **32**, 7-14 (2019). https://doi.org/10.1089/vim.2018.0085

68 Murira, A. & Lamarre, A. Type-I Interferon Responses: From Friend to Foe in the Battle against Chronic Viral Infection. *Frontiers in immunology* **7**, 609 (2016). https://doi.org/10.3389/fimmu.2016.00609

69 Levine, A. J. *et al.* Systems analysis of human brain gene expression: mechanisms for HIV-associated neurocognitive impairment and common pathways with Alzheimer's disease. *BMC Med Genomics* **6**, 4 (2013). https://doi.org/10.1186/1755-8794-6-4

70 Esiri, M. M., Morris, C. S. & Millard, P. R. Fate of oligodendrocytes in HIV-1 infection. *AIDS* **5**, 1081-1088 (1991). https://doi.org/10.1097/00002030-199109000-00003

71 Kaalund, S. S., Johansen, A., Fabricius, K. & Pakkenberg, B. Untreated Patients Dying With AIDS Have Loss of Neocortical Neurons and Glia Cells. *Front Neurosci* **13**, 1398 (2019). https://doi.org/10.3389/fnins.2019.01398

72 Colonna, M. & Butovsky, O. Microglia Function in the Central Nervous System During Health and Neurodegeneration. *Annual review of immunology* **35**, 441-468 (2017). https://doi.org/10.1146/annurev-immunol-051116-052358

73 Lee, H. G., Lee, J. H., Flausino, L. E. & Quintana, F. J. Neuroinflammation: An astrocyte perspective. *Science translational medicine* **15**, eadi7828 (2023). https://doi.org/10.1126/scitranslmed.adi7828

74 Aisenberg, W. H. *et al.* Direct microglia replacement reveals pathologic and therapeutic contributions of brain macrophages to a monogenic neurological disease. *Immunity* **58**, 1254-1268 e1259 (2025). https://doi.org/10.1016/j.immuni.2025.03.019

75 Bennett, F. C. *et al.* A Combination of Ontogeny and CNS Environment Establishes Microglial Identity. *Neuron* **98**, 1170-1183 e1178 (2018). https://doi.org/10.1016/j.neuron.2018.05.014

76 Chadarevian, J. P. *et al.* Harnessing human iPSC-microglia for CNS-wide delivery of disease-modifying proteins. *Cell Stem Cell* **32**, 914-934 e918 (2025). https://doi.org/10.1016/j.stem.2025.03.009

77 Chadarevian, J. P. *et al.* Therapeutic potential of human microglia transplantation in a chimeric model of CSF1R-related leukoencephalopathy. *Neuron* **112**, 2686-2707 e2688 (2024). https://doi.org/10.1016/j.neuron.2024.05.023

78 Chadarevian, J. P. *et al.* Engineering an inhibitor-resistant human CSF1R variant for microglia replacement. *J Exp Med* **220** (2023). https://doi.org/10.1084/jem.20220857

79 Han, X. *et al.* Forebrain engraftment by human glial progenitor cells enhances synaptic plasticity and learning in adult mice. *Cell Stem Cell* **12**, 342-353 (2013). https://doi.org/10.1016/j.stem.2012.12.015

80 Mancuso, R. *et al.* Stem-cell-derived human microglia transplanted in mouse brain to study human disease. *Nat Neurosci* **22**, 2111-2116 (2019). https://doi.org/10.1038/s41593-019-0525-x

81 Rathinam, C. *et al.* Efficient differentiation and function of human macrophages in humanized CSF-1 mice. *Blood* **118**, 3119-3128 (2011). https://doi.org/10.1182/blood-2010-12-326926

82 Serneels, L. *et al.* A versatile mouse model to advance human microglia transplantation research in neurodegenerative diseases. *Mol Neurodegener* **20**, 29 (2025). https://doi.org/10.1186/s13024-025-00823-2

83 Shibuya, Y. *et al.* Treatment of a genetic brain disease by CNS-wide microglia replacement. *Sci Transl Med* **14**, eabl9945 (2022). https://doi.org/10.1126/scitranslmed.abl9945

84 Vieira, R. *et al.* Young glial progenitor cells competitively replace aged and diseased human glia in the adult chimeric mouse brain. *Nat Biotechnol* **42**, 719-730 (2024). https://doi.org/10.1038/s41587-023-01798-5

85 Windrem, M. S. *et al.* Neonatal chimerization with human glial progenitor cells can both remyelinate and rescue the otherwise lethally hypomyelinated shiverer mouse. *Cell Stem Cell* **2**, 553-565 (2008). https://doi.org/10.1016/j.stem.2008.03.020

86 Windrem, M. S. *et al.* A competitive advantage by neonatally engrafted human glial progenitors yields mice whose brains are chimeric for human glia. *J Neurosci* **34**, 16153-16161 (2014). https://doi.org/10.1523/JNEUROSCI.1510-14.2014

87 Yoo, Y., Neumayer, G., Shibuya, Y., Mader, M. M. & Wernig, M. A cell therapy approach to restore microglial Trem2 function in a mouse model of Alzheimer's disease. *Cell stem cell* **30**, 1043-1053 e1046 (2023). https://doi.org/10.1016/j.stem.2023.07.006

88 Wahl, A. & Al-Harthi, L. HIV infection of non-classical cells in the brain. *Retrovirology* **20**, 1 (2023). https://doi.org/10.1186/s12977-023-00616-9

89 Tang, Y. *et al.* Brain microglia serve as a persistent HIV reservoir despite durable antiretroviral therapy. *The Journal of clinical investigation* **133** (2023). https://doi.org/10.1172/JCI167417

90 Ash, M. K., Al-Harthi, L. & Schneider, J. R. HIV in the Brain: Identifying Viral Reservoirs and Addressing the Challenges of an HIV Cure. *Vaccines (Basel)* **9** (2021). https://doi.org/10.3390/vaccines9080867

91 Lia, A. *et al.* Rescue of astrocyte activity by the calcium sensor STIM1 restores long-term synaptic plasticity in female mice modelling Alzheimer's disease. *Nature communications* **14**, 1590 (2023). https://doi.org/10.1038/s41467-023-37240-2

92 Michaelis, M., Nieswandt, B., Stegner, D., Eilers, J. & Kraft, R. STIM1, STIM2, and Orai1 regulate store-operated calcium entry and purinergic activation of microglia. *Glia* **63**, 652-663 (2015). https://doi.org/10.1002/glia.22775

93 Serwach, K. & Gruszczynska-Biegala, J. Target Molecules of STIM Proteins in the Central Nervous System. *Front Mol Neurosci* **13**, 617422 (2020). https://doi.org/10.3389/fnmol.2020.617422

94 Alexander, D. C. *et al.* Targeting acetyl-CoA metabolism attenuates the formation of fear memories through reduced activity-dependent histone acetylation. *Proceedings of the National Academy of Sciences of the United States of America* **119**, e2114758119 (2022). https://doi.org/10.1073/pnas.2114758119

95 Mews, P. *et al.* Alcohol metabolism contributes to brain histone acetylation. *Nature* **574**, 717-721 (2019). https://doi.org/10.1038/s41586-019-1700-7

96 Mews, P. *et al.* Acetyl-CoA synthetase regulates histone acetylation and hippocampal memory. *Nature* **546**, 381-386 (2017). https://doi.org/10.1038/nature22405

97 Bernardo, A., Agresti, C. & Levi, G. HIV-gp120 affects the functional activity of oligodendrocytes and their susceptibility to complement. *J Neurosci Res* **50**, 946-957 (1997). https://doi.org/10.1002/(SICI)1097-4547(19971215)50:6<946::AID-JNR5>3.0.CO;2-D

98 Marino, J. *et al.* Functional impact of HIV-1 Tat on cells of the CNS and its role in HAND. *Cell Mol Life Sci* **77**, 5079-5099 (2020). https://doi.org/10.1007/s00018-020-03561-4

99 Zou, S. *et al.* Oligodendrocytes Are Targets of HIV-1 Tat: NMDA and AMPA Receptor-Mediated Effects on Survival and Development. *J Neurosci* **35**, 11384-11398 (2015). https://doi.org/10.1523/JNEUROSCI.4740-14.2015

100 Falcao, A. M. *et al.* Disease-specific oligodendrocyte lineage cells arise in multiple sclerosis. *Nature medicine* **24**, 1837-1844 (2018). https://doi.org/10.1038/s41591-018-0236-y

101 Kaya, T. *et al.* CD8(+) T cells induce interferon-responsive oligodendrocytes and microglia in white matter aging. *Nat Neurosci* **25**, 1446-1457 (2022). https://doi.org/10.1038/s41593-022-01183-6

102 Kirby, L. *et al.* Oligodendrocyte precursor cells present antigen and are cytotoxic targets in inflammatory demyelination. *Nature communications* **10**, 3887 (2019). https://doi.org/10.1038/s41467-019-11638-3

103 Abud, E. M. *et al.* iPSC-Derived Human Microglia-like Cells to Study Neurological Diseases. *Neuron* **94**, 278-293 e279 (2017). https://doi.org/10.1016/j.neuron.2017.03.042

104 Mestas, J. & Hughes, C. C. Of mice and not men: differences between mouse and human immunology. *J Immunol* **172**, 2731-2738 (2004). https://doi.org/10.4049/jimmunol.172.5.2731

105 Pardridge, W. M. Blood-Brain Barrier and Delivery of Protein and Gene Therapeutics to Brain. *Front Aging Neurosci* **11**, 373 (2019). https://doi.org/10.3389/fnagi.2019.00373

106 Zhou, D., Zhu, X. & Xiao, Y. Advances in CAR-T therapy for central nervous system tumors. *Biomark Res* **12**, 132 (2024). https://doi.org/10.1186/s40364-024-00679-6

107 McCarthy, K. D. & de Vellis, J. Preparation of separate astroglial and oligodendroglial cell cultures from rat cerebral tissue. *J Cell Biol* **85**, 890-902 (1980). https://doi.org/10.1083/jcb.85.3.890

108 Keele, B. F. *et al.* Identification and characterization of transmitted and early founder virus envelopes in primary HIV-1 infection. *Proceedings of the National Academy of Sciences of the United States of America* **105**, 7552-7557 (2008). https://doi.org/10.1073/pnas.0802203105